Evidence for seawater Mg/Ca and dietary control on Mg incorporation in oyster shells.

Marie Pesnin[1,2*], Laurent Emmanuel[2], Amélie Guittet[2], Boris Eyheraguidel[3], Gaëtan Schires[4], Julien Normand[5], Vincent Mouchi[6]

[1]: Geowissenschaftliches Zentrum, Georg–August–Universität Göttingen, 37077, Göttingen, Germany.

[2]: Sorbonne Université, CNRS-INSU, Institut des Sciences de la Terre Paris, ISTeP, F-75005, Paris, France

[3]: Institut de Chimie de Clermont-Ferrand, Campus universitaire des Cézeaux, 63178, Aubière, France

[4]: Station Biologique de Roscoff, CNRS-Sorbonne Université, Roscoff 29682, France.

[5]: Ifremer, Laboratoire Environnement Ressources de Normandie, Avenue du Général de Gaulle, 14520, Port-en-Bessin, France

[6]: CNRS, CReAAH, Université de Rennes, Campus Beaulieu, 263 avenue Général Leclerc, 35042, Rennes Cedex, France

[*]Corresponding author: marie.pesnin@uni-goettingen.de

This is a reviewed manuscript that has been accepted for publication in Chemical Geology

Abstract

The Mg/Ca ratio in bivalve shells has been investigated as a promising proxy for temperature reconstruction of the seawater. However, important discrepancies exist among the Mg/Ca-temperature calibrations reported for bivalves in the literature. These discrepancies currently limit the use of Mg/Ca for paleoclimate reconstructions based on bivalves and suggest that factors beyond temperature influence Mg incorporation in the shell. In particular, several studies have highlighted empirical differences in the seasonal amplitudes of shell Mg/Ca between two types of environments: river-influenced coastal settings and open marine systems. In this study, we investigate several environmental parameters that may account for these differences, using rearing experiments of oysters in both natural and artificial seawater. First, we tested the influence of Mg speciation in seawater on shell Mg/Ca and showed that Mg is incorporated in the shell regardless of its form (free or complexed with organics). Second, we investigated the sensitivity of shell Mg/Ca to seawater Mg/Ca by artificially increasing the Mg concentration in seawater. We observed an increase in shell Mg/Ca concomitant with the rise in seawater Mg/Ca, confirming the dependance of shell Mg/Ca on seawater Mg content. Finally, we show that a change in diet induces a significant difference in shell Mg/Ca, and that shell Mg/Ca is positively correlated with the Mg/Ca of the diet. Overall, our results suggest that, in addition to temperature, both seawater and dietary Mg/Ca ratios control shell Mg/Ca. These parameters could be responsible for the discrepancy between Mg/Ca-temperature models published in the literature, and should be carefully considered in future aquarium-based and in situ calibration studies, as well as paleoenvironmental reconstructions.

Keywords: Mg bioavailability, Mg/Ca ratio, Bivalves, Complexed Mg, Diet.

1. Introduction

Present-day climates are defined by both the mean values and variabilities of environmental parameters over a period of 30-years (WMO, 2025). Reconstructing past climates therefore requires paleoenvironmental archives with compatible temporal resolution. Unlike sedimentary records, climatic cycles within the carbonate shell of marine molluscs occur with a temporal resolution ranging from multi-annual to tidal scales (Chauvaud et al., 2005; Lartaud et al., 2010a; Huyghe et al., 2019; Mouchi et al., 2025a). The investigation of such high-frequency paleoenvironmental archives is essential to improve the temporal resolution of paleoclimate models and thus better anticipate future environmental changes. Bivalves can record, within their shells, variations in physicochemical parameters governing their living environment such as temperature (e.g., Epstein et al, 1953; Purton and Brasier, 1997; Kirby et al., 1998; Vander Putten et al., 2000; Mouchi et al., 2013; Huyghe et al., 2015, Briard et al., 2020; Uvanovic et al., 2021). Traditionally, paleoclimatologists have relied on oxygen isotope ratios ($\delta^{18}O$) of calcium carbonate shells to access past seawater temperatures. However, the $\delta^{18}O$ of calcium carbonate is known to not only depend on the temperature but also on the $\delta^{18}O$ of the seawater from which it forms (e.g., Urey et al., 1951, Epstein et al, 1953). In costal environments, the $\delta^{18}O$ of the seawater is particularly difficult to constrain due to seasonal variations of the freshwater inputs, complicating the interpretation of bivalve $\delta^{18}O$ records (Rohling, 2000; Pierre, 1999).

Alternative geochemical proxies, dependent solely on temperature, are therefore being investigated to faithfully reconstruct seawater temperature variations in coastal environments. Among these, the Mg/Ca ratio bivalve shells have been widely studied as a potential temperature proxy (e.g., Klein et al., 1996; Vander Putten et al., 2000; Surge & Lohmann, 2008; Bougeois et al., 2016; Tynan et al., 2017; Mouchi et al., 2018, Hausmann et al., 2024). However, this paleo-climatic proxy is also known to be controlled by other factors (e.g., pH and specimen age; Lazareth et al., 2007; Surge & Lohmann, 2008; Mouchi et al., 2013; Schöne & Gillikin, 2013; Hausmann et al., 2017), making its interpretation in terms of climatic conditions challenging. In particular, large variability has been reported in both shell Mg/Ca absolute values and sensibility of shell Mg/Ca to temperature (Freitas et al., 2008; Wanamaker et al., 2008; Tynan et al., 2017; Mouchi et

al., 2018; Schleinkofer et al., 2021; Mouchi et al., 2025b; **Figure 1**). While salinity has generally been shown to have a limited effect on shell Mg/Ca (Mouchi et al., 2013), previous studies have highlighted systematic differences between Mg/Ca values in shells from open marine and estuarine or bay environments (Mouchi et al., 2018; **Figure 1**). Since Mg^{2+} is one of the most abundant cations in seawater, its availability should be increased in open marine settings compared to coastal areas where seawater is diluted by freshwater input. However, observations indicate that estuarine bivalves present a higher Mg/Ca than those of marine settings (Mouchi et al., 2018). Several hypotheses have been advanced to explain this discrepancy.

One potential explanation could be that the Mg/Ca of the shell also varies depending on the Mg/Ca of the seawater, which itself varies depending on the environments (Tynan et al., 2017). Another possibility could be the bio-availability of Mg. Mg in seawater exists in two forms: free Mg^{2+} and complexed Mg. Magnesium is considered free in seawater when it is not bound with other ions or ligands, although it constantly interacts with six water molecule that constitute its inner hydration sphere. In contrast, complexed Mg forms covalent bonds with inorganic ligands (e.g., OH^-, SO_4^{2-}, PO_4^{2-}, CO_3^{2-}, HCO_3^-, Cl^-) or organic ligands (e.g., carboxylic acids, carbohydrates, amino acids, phenolic compounds) (Hirose. 2006). Although the nature and origin of the organic ligands remains largely unknown, by analogy with Fe, the organic ligands can be classified into two main groups: those produced by photosynthetic organisms (chlorophylls) and those derived from the degradation of organic matter (Chipmann, 1966; Marchand et al., 1974; Hunter and Boyd, 2007). The proportion of the two forms of Mg in seawater has never been directly measured. Indeed, conventional methods for measuring Mg in seawater, which generally involve plasma ionization (ICP-OES, ICP-AES, ICP-MS; Surge & Lohmann, 2008; Tynan et al., 2017), quantify the total Mg in a solution, regardless of its form. Nevertheless, studies have shown a positive gradient of dissolved organic matter concentration in seawater from estuarine to open marine environments (Le Corre et al., 1972; Wafar and Le Corre, 1982, Zhang et al., 2019). It is accepted that the greater the abundance of organic ligands in a medium, the more favorable the medium becomes for the formation and preservation of organometallic complexes (Zhang et al., 2019). Thus, we can assume that seawater in open marine environments is richer in complexed Mg than that in estuarine environments. The experimental work of Mavromatis et al. (2017)

demonstrated that the presence of Mg-organic complexes enhances Mg incorporation into abiotic calcite via surface adsorption mechanisms. However, the effect of such organic ligands on Mg incorporation into biogenic calcite remains unknown. It is possible that their impact differs significantly in biological systems. In particular, Mg complexed with organic ligands is likely less bioavailable because it must first be transported across cell membranes and undergo enzymatic decomposition to release free Mg^{2+} ions (Shaked & Lis, 2012). These enzymatic processes are energetically costly, and bivalves may preferentially incorporate free Mg^{2+} ions from seawater, which requires less energy. An alternative hypothesis to explain the high shell Mg/Ca in estuarine settings compared to open marine would be the food source, if Mg content is higher depending on the plankton species.

To test these hypotheses and better assess the bioavailability of Mg in seawater for bivalves, we conducted a 7-month rearing experiment using the oyster *Magallana gigas*. We chose oysters for this experiment because of their rapid growth and good shell preservation potential (Mouchi et al., 2025a). We tested the influence of three sources of Mg on its incorporation in *M.gigas* shells: (1) Free Mg^{2+}, (2) Complexed Mg with strong organic ligand (ETDA), and (3) Mg from dietary sources. The chemical composition of the shells was analysed in situ using laser ablation-inductively coupled plasma mass spectrometry (LA-ICP-MS). The Mg concentrations in these shells were compared between treatments to identify the preferred source of the Mg incorporated into the shells. Overall, the results of this experiment contribute to a better use of the Mg/Ca proxy by providing new constrains on factors beyond temperature that control Mg incorporation in bivalve shells.

2. Materials

2.1. *Magallana gigas* specimens

The rearing experiment was performed on specimens of *Magallana gigas*. These oysters, originating from spatfall, had initially been reared in the Baie des Veys (49°22’35" N, 1°08’20" W) in the southern English Channel. A total of 300 one-year-old individuals were collected alive and transferred to aerated seawater tanks to ensure their survival during transportation to the rearing sites. The individuals were then randomly assigned to one of two culture sites of Sorbonne University: Biological Station of Roscoff (SBR,

Roscoff Aquarium Services) and the Institute of Earth Sciences of Paris (ISTeP). The oysters were maintained in natural seawater (NSW) at Roscoff, while they were reared in artificial seawater (ASW) at Paris. Each oyster was labelled with a unique identification number using micro-labels affixed to the shell (Hallprint Glue-on Shellfish Tags type FPN 8x4 mm), with specimens in natural seawater (Roscoff) numbered G.000 to G.150 and those in artificial seawater (Paris) numbered G.300 to G.450 (see **Supplementary data 1, Figure S1**). We allowed the oysters to acclimatise to the laboratory breeding conditions for two weeks before starting the experiment.

2.2. Rearing strategy

2.2.1. General settings

Three tanks with a capacity of 30 liters at Paris (P1, P2, P3) and 100 liters at Roscoff (R1, R2/R4, R3) were set up to accommodate *M. gigas* individuals collected on the field (**Figure 2**). At Roscoff, the tanks were filled with natural seawater (NSW) pumped from offshore (48°72'N, 3°98'W), while at Paris, tanks were supplied with artificial seawater (ASW) prepared by dissolving Instant Ocean® synthetic sea salt into deionized water produced by reverse osmosis. The amount of Instant Ocean salt added to the solution was chosen to achieve a salinity of 35, consistent with the NSW at Roscoff. Furthermore, to minimize salinity fluctuations due to evaporation, perforated lids were placed on the top of each tank at the Paris rearing site (**Figure 2a**). Twice a week, 10% to 17% of the ASW and NSW was renewed to maintain a stable Mg concentration. In addition, complete water renewal and tank cleaning were performed monthly in Paris to remove organic waste and prevent nitrite accumulation. To ensure proper water oxygenation of the ASW, all tanks were equipped with aeration and circulation systems (**Figure 2a**). Water flow was programmed to follow a day/night cycle to mimic natural fluctuations (2 tidal cycles per day). In contrast, at the Roscoff site, water circulation was achieved through a two-level mechanical overflow system (**Figure 2b**). This system allowed water to flow from the rearing aquarium to a recovery tank equipped with pre-colonized bacterial filter, from which seawater was pumped back to the rearing aquarium.

To stabilize seawater temperature during the experimental period, the rearing tank were installed in air-conditioned room. Tank's seawater temperature was maintained at ~ 20°C corresponding to the temperature range at which discrepancies between published Mg/Ca–temperature calibrations are most pronounced (**Figure 1**).

Each tank initially received 30 *M. gigas* oysters, with additional specimens maintained in holding tanks to replace any that died during the experiment. All oysters - except those in tank R4 - were fed daily with 1 mL of concentrated Instant Algae© Shellfish Diet 1800, a mixed microalgae culture containing *Tetraselmis* sp., *Thalassiosira weissflogii*, and *Thalassiosira pseudonana* (all <20 µm in size).

Immediately, at the beginning of the experiment, in vivo Mn labeling of all specimens was performed to locate the experimental period in the shell, following the protocol described in Lartaud et al. (2010). Specimens were introduced into a temporary tank filled with seawater enriched in $MnCl_2$ (total concentration: 90 $mg.L^{-1}$) for 4.5h. Additional Mn labels were performed throughout the experimental period (**Supplementary data 2 and 3**) to follow shell growth.

2.2.2. Experimental conditions

At each site, in addition to a control tank, two experimental tanks were used to test the effect of different Mg sources on the shell Mg/Ca record (**Figure 3a**).

2.2.2.1. Seawater enriched with Mg

To assess whether the Mg concentration in seawater influences the Mg/Ca ratio of *M. gigas* shells, tanks P2 (Paris, ASW) and R2 (Roscoff, NSW) were artificially enriched with 5.22 mmol of Mg compared to control tanks (P1 and R1) (**Figure 3a**). To maintain this enrichment, a solution of $MgCl_2$ (99% anhydrous magnesium chloride) was prepared in 100 mL of artificial seawater (or natural seawater at Roscoff) and added to the aquariums during each water renewal. An additional condition was introduced later in the year (April 2, 2021), at the Paris site, in tank P3, where the Mg concentration was further increased to 10.44 mmol, while the conditions in P2 remained unchanged (**Figure 3**).

2.2.2.2. Seawater enriched with EDTA-Mg complexes

To examine the role of magnesium organic complexes, tank R3 at Roscoff was enriched with 5.22 mmol of complexed Mg by adding a magnesium-EDTA solution (TCI, ref. E0094) during each water renewal (**Figure 3a**).

2.2.2.3. Different food supply

To investigate whether diet affects shell Mg/Ca, the oyster's feeding regimen in tank R2 was modified, establishing a new experimental referred to as R4 (**Figure 3**). In practice, on March 5, 2021, Mg enrichment was stopped and the R2 tank was emptied, thoroughly rinsed, and refilled with filtered natural seawater. From that point onward, oysters in this tank were fed with a fresh mono-specific culture of *Skeletonema* sp., a diatom species naturally consumed by oysters (Pouil et al., 2020), grown at the Roscoff Biological Station. The Mg content of the *Skeletonema. sp* culture was analyzed by inductively coupled plasma optical emission spectrometry (ICP-OES) and compared to that of the *Instant Algae* used in other tanks.

2.2.2.4. Control conditions

Control tanks (P1 and R1) did not receive any artificial Mg enrichment. *M. gigas* individuals raised in these tanks were maintained under the same environmental conditions (temperature and salinity) and feeding regimen (i.e, *Instant Algea*) as those in the experimental tanks (except R4), enabling direct comparison between conditions.

2.2.3. Monitoring of rearing conditions

The rearing experiment started on October 28, 2020, at the Paris site and on November 16, 2020 at Roscoff (**Figure 3b**)**.** Throughout the 7-month experimental period, daily monitoring of seawater temperature, salinity, and oyster mortality was performed for each tank (**Supplementary data 2 and 3**). Seawater samples were regularly collected to monitor Mg enrichment levels and assess the impact of water renewal on Mg concentrations. In addition, shell growth was tracked using in vivo Mn^{2+} labeling and cathodoluminescence imaging,

3. Methods

3.1. Shell sample preparation and location of Mn markings

Magallana gigas specimens were removed from rearing tanks at various stages of the culture experiment for geochemical analysis. Immediately after collection, the oysters were opened, their soft tissues were removed, and the shells were rinsed with deionized water. To ensure shell preservation and eliminate residual organic matter, shells were immersed overnight in a 15% hydrogen peroxide (H_2O_2) solution and then thoroughly rinsed with demineralized water.

For geochemical analysis, we focused on the hinge area rather than the whole shell, as it preserves the organism's growth history within a single, well-defined portion (Langlet et al., 2006; Lartaud et al., 2010a). The umbo of each left valve was removed and embedded in Huntsman Araldite 2020 epoxy resin. A longitudinal thick section was then cut along the maximum growth axis, from the hinge region to the ventral shell margin, revealing growth increments. The resulting thin sections were polished to a final thickness of ~300 µm using alumina powder. All geochemical analyses were performed on the foliated calcite layer within the hinge sections.

To locate Mn markings withing *M. gigas* shells, cathodoluminescence (CL) microscopy was carried out following the method described in Lartaud et al. (2010). CL observations were conducted at ISTeP using a cold cathode (Cathodyne-OPEA) under operating conditions of 15–20 keV and 200–400 µA.mm^{-2} at a pressure of 0.05 Torr. Luminescence images were captured with a Nikon D500 camera (ISO 1400) using a 20-second exposure time. In calcite, Mn^{2+} incorporation during mineral growth produces a characteristic CL emission at ~620 nm, observed as bright red luminescence (**Figure 4a**). Mn markings identified by CL microscopy were cross-referenced with Mn content variations measured by LA-ICP-MS (**Figure 4b**). Since growth of the umbo reflects overall shell growth (Lartaud et al., 2010a), the timing of Mn markings, combined with CL observations, was used to estimate shell growth rates under rearing conditions (**Supplementary data 1, Table S2**).

3.2. Geochemical analyses

3.2.1. Elemental concentration in seawater

In order to determine the form of Mg in seawater, we combined two analytical techniques commonly used to characterize seawater chemistry: inductively-coupled plasma optical emission spectrometry (ICP-OES) and ion chromatography (IC). ICP-OES involves introducing the sample into a very high-temperature plasma, which completely dissociates chemical complexes and organic compounds, thereby allowing the quantification of total Mg in solution regardless of its initial chemical form. In contrast, ion exchange chromatography separates and detects dissolved species based on their charge and interactions with an ion-exchange resin, thus limiting the measurement to free Mg present in solution. The combination of these two approaches therefore allows the fraction of complexed Mg to be estimated by comparing the total Mg concentration measured by ICP-OES with the concentration of free Mg determined by ion chromatography.

3.2.1.1. Quantification of total Mg in seawater

Natural and artificial seawater samples were regularly collected from each aquarium and analyzed using inductively coupled plasma optical emission spectrometry (ICP-OES) to assess Mg and Ca elemental concentration. On average, 25 mL of water was sampled from each aquarium once per month, just before water renewal and oyster feeding. In addition, a one-week daily monitoring (morning and afternoon) of Mg concentration in ASW at the Paris rearing site was conducted to evaluate the impact of aquarium artificial seawater renewal on Mg concentration (**Supplementary data 4**). Immediately after collection, seawater samples were acidified with 30 µL of nitric acid (HNO_3, 68% Normapur) and stored at +2°C in the dark until analysis. To differentiate between free and complexed form of Mg, each sample was divided into two aliquots: one was filtered using a 2 µm Whatman 540 filter and diluted 1:200 in a 2% HNO_3 solution prepared with deionized water (resistivity: 18 MΩ·cm) for ICP-OES analysis, while the second aliquot was kept for free Mg quantification by ion exchange chromatography (IC).

To further evaluate Mg input from the oyster diet (*Instant Algae / Skeletonema*), the elemental composition of daily nutritional solutions used to feed *M. gigas* was also analysed by ICP-OES. Approximately 5 mL of each solution was mineralized in 5 mL of 68% HNO_3 under continuous agitation for 12 hours to release intracellular elements. The solution was then filtered through a 2 µm Whatman 541 filter to confirm the absence of residual cellular material. If incomplete mineralization was observed, the solution was first diluted with deionized water and the mineralization process was repeated. Fully processed samples were subsequently diluted in a 2% HNO_3 to a final dilution factor of 1:256 and stored with seawater samples at +2°C in the dark until analysis.

Elemental measurements were performed using an Agilent ICP-OES 5100 SVDV at the ALLIP6 analytical platform (Sorbonne University). Calibration was established using four standard solutions of known elemental concentrations, which were analyzed before and after all sample sequences to correct for potential instrumental drift and convert intensity signal to concentration. Standards were additionally analyzed after every 20 samples to monitor potential contamination. Blank samples were prepared and analyzed alongside experimental samples to verify the absence of contamination from reagents. A full ICP-OES analysis report is available in **Supplementary data 5**.

3.2.1.2. Quantification of organic Mg complexes in seawater

The amount of Mg complexed in seawater was determined by combining measurements of total Mg (obtained by ICP-OES) and free Mg^{2+} (obtained by ion-exchange chromatography).

IC analyses were conducted at the Institute of Chemistry of Clermont-Ferrand (ICCF) using a Dionex ICS-6000 HPIC™ system equipped with a 2 × 250 mm IC column (Dionex IonPac™ CS-16). The Mg^{2+} concentration in eluted seawater samples was quantified via mass spectrometry using an ISQ™ EC Single Quadrupole Mass Spectrometer. Data acquisition and processing were performed using Chromeleon 7.2 software. Analytical reproducibility was assessed from three replicates for each water sample (**Supplementary data 6**).

IC analyses were conducted on both natural (R1, R2, and R4) and artificial (P1, P2, P3) seawater. However, due to the incompatibility of ethylenediaminetetraacetic acid (EDTA) with ion chromatography (Sharpe and London, 1997; Chumanov and Burgess, 2011), IC could not be performed on seawater samples from R3.

Prior to IC analysis, seawater samples were acidified and diluted 1:3000 in deionized water. These two steps in sample preparation are very likely to destabilize inorganic magnesium complexes such as $MgOH^+$, $MgSO_4^0$, and $MgHCO_3^+$ potentially present in solution, causing the the release of extra Mg^{2+} in the dissolved free Mg pool. As a result, the Mg^{2+} concentration measured by IC reflects both the free Mg^{2+} originally present in solution and Mg from inorganic complexes.

The concentration of organically complexed Mg (hereafter referred as $Mg_{organic\ complexed}$) was then calculated by subtracting the contribution of free Mg^{2+} and Mg released from inorganic complexes (hereafter referred as $\sum(Mg_{free,}\ Mg_{inorganic\ complexes})$) to the total Mg concentration (hereafter referred as Mg_{tot})) measured by ICP-OES.

3.2.2. Shells elemental concentration by LA-ICP-MS

Elemental compositions of oyster shells were analyzed by laser-ablation inductively-coupled plasma mass spectrometry (LA-ICP-MS) at the Centre de Recherche en Archéologie, Archéosciences, Histoire (CReAAH, Université de Rennes, UMR 6566). Additional specimens were analysed at the Institut des Sciences Analytiques et de Physico-Chimie pour l'Environnement et les Matériaux (IPREM, Université de Pau et des Pays de l'Adour). At CReAAH, analyses were performed using an Agilent Technologies 7700 Series ICP-MS coupled with a Cetac Technologies LSX-213 G2 laser ablation system (213 nm). A total of 29 oyster shells were analyzed, including specimens that experienced different environmental conditions along growth (**Table 1,** see also **Table S2** in **Supplementary data 1**), separated by *in vivo* Mn-labelling. Analytical transects were performed to cross all Mn labels (observed with cathodoluminescence) using laser parameters as 25 µm spot size, 10 Hz frequency, 23 µJ energy, and a scanning speed of

10 µm.s^{-1}. At IPREM, an Agilent 8900 ICPMS Triple Quad was used, coupled with a femtosecond laser ablation system (Novalase SA), equipped with a 2D galvanometric scanner which allows the 15 µm laser beam to move at high speed (1 mm.s^{-1}). Laser parameters for 20 µm-wide transects were 200 Hz frequency, 23 µJ energy, and 5 µm.s^{-1} scanning speed. Measured elements were ^{24}Mg, ^{55}Mn and ^{43}Ca as internal standard. Reference materials NIST SRM 610, 612 and 614 were analyzed at the start, middle and end of each analytical session for calibration. Accuracy was checked using repeated measurements of certified otolith reference materials FEBS-1 and NIES-22, with preferred values of the GeoReM database (Jochum et al., 2005), when available. Data reduction for CReAAH analyses was performed on Matlab (http://www.mathworks.com) following the procedure described by Longerich et al. (1996) while IPREM data was processed with an equivalent procedure using an inhouse software FOCAL v. 2.46.

3.2.3. Data processing

Data processing was performed using Matlab (v. R.2023b; http://www.mathworks.com). Experimental condition intervals along Mg/Ca transects were identified by localizing the *in vivo* labels from the Mn/Ca profiles. To prevent potential influence from preceding conditions, the analytical point corresponding to the first label of each condition was excluded from the final dataset. The total number of retained analytical points was 1634. As each treatment was represented by a single experimental tank, inferential statistical comparisons among treatments could not be performed due to the lack of replicates among treatments (pseudoreplication). Consequently, all results are presented descriptively.

4. Results

4.1. Monitoring of seawater physicochemical parameters

The average temperature and salinity values for each rearing condition are reported in **Table 2.** Over the seven-month experimental period, we observed fluctuation of seawater temperature between 18°C and 22°C at the Paris site, and between 17°C and 24°C at the Roscoff site (**Supplementary data 1, Figure S2 and S3**). These temperature fluctuations do not follow a clear seasonal trend and are likely attributable to variations in the efficiency of the room's air conditioning systems. Although temperature changes occur

synchronously across the three tanks at each site, statistical analyses reveal consistent differences in mean temperature between individual tanks: at the Paris rearing site, tank P3 consistently exhibit a mean temperature 0.7°C higher than tanks P1 and P2, while at Roscoff, tank R3 shows a mean temperature 0.7°C lower than tanks R1 and R2/R4 (**Table 2**).

Our experimental setup mimic an open marine environment in that no continental inputs are present. In such environmental settings and based on published thermodependent Mg/Ca models (Mouchi et al., 2013), a 0.7°C temperature shift is expected to result in a change of 0.31 $mmol.mol^{-1}$ in shell Mg/Ca. This change, however, remains negligible compared to the differences in shell Mg/Ca observed between experimental conditions (2.65 $mmol.mol^{-1}$ between P1 and P3 and 7.07 $mmol.mol^{-1}$ between R1 and R3, **Table 2**).

At the Paris site, salinity fluctuations ranged from 32 to 40 psu, with an average of 35.1 psu. The most pronounced variations of salinity were associated to the complete renewal of tank water (**Supplementary data 2**). In addition, tank P2 showed 1 psu higher salinity than P1, which is consistent with the Mg enrichment it received (**Table 2**). Conversely, tank P3 does not exhibit higher salinity than P2, despite receiving a theoretically greater Mg enrichment.

4.2. Growth rates and mortality

Over the seven-month experiment, mortality remained low across all rearing conditions, except in R3, which received EDTA treatment. In conditions P1, P2, P3, R1, R2/R4, the first mortalities occured after six months and gradually increased toward the end of the rearing period (**Supplementary data 1, Figure S4**). In contrast, R3 exhibited a sharp increase in mortality, with 35.7% of oysters died by day 35 of experiment and all *M. gigas* specimens were dead within the following 10 days.

Based on CL observations, we found that, over the entire experimental period, the growth rate of the *M. gigas* umbos varied between 0.14 and 3.03 $\mu m.day^{-1}$ across individuals (**Supplementary data 1, Table S1**). **Figure 5** present a comparison of the *M.gigas* growth between the experimental conditions. For identical rearing conditions,

426 growth-rate distributions largely overlap between oysters reared in artificial and natural
427 seawater, both for P1–R1 and P2–R2 comparisons (**Figure 5**). Although growth rates tend
428 to be slightly higher under R2 compared to P2, these results indicate seawater type
429 (artificial or natural) has no effect on shell growth. Likewise, no clear effect of seawater
430 Mg concentration in seawater on shell growth is observed. Oysters reared in artificial
431 seawater exhibit comparable growth rates between P1 and P2, while thoses reared under
432 condition P3 show slitly lower growth rates (**Figure 5**). Conversaly, oysters reared under
433 Mg-enriched conditions in natural seawater (R2) tend to show higher growth rates than
434 those reared under control condition (R1). These contradictory observation suggest that
435 changes in seawater Mg concentration between conditions are unlikely to be a major
436 factor in this study. In contrast, oysters reared under condition R3, where Mg
437 enrichement of the seawater was achieved by adding Mg-EDTA, showed a dractic
438 reduction in growth rate of approximately 50% compared to control condition R1. Finally,
439 diet appears to have a small effect on oyster growth, with oysters fed Skeletonema (R4)
440 showing, on average, higher growth rates than those fed Instant Algae (R1) (**Table 2**).
441
442 Periodic Mn labelling in oysters from P1 and P2 allowed further assessment of growth
443 rate evolution through the experimental period (**Supplementary data 1, Figure S7**).
444 Although some inter-individual variability was observed, the overall trend reveals a
445 gradual decline in *M. gigas* growth rate throughout the experiment, decreasing from an
446 average of 2-3 mm day^{-1} at the beginning of the incubation to less than 1 mm day^{-1} by the
447 end of the experiment. This decline coincides with increasing mortality toward the end of
448 the experiment, and may be linked to inadequate feeding of the oyster, either due to poor
449 food quality or insufficient daily food ration delivered to the tanks.
450
451 **4.3. Concentration and form of Mg in the oyster rearing environment.**

452 ***4.3.1. Total Mg in natural and artificial seawater***

453 Total Mg and Ca concentrations in aquarium seawater measured by ICP OES range
454 from 51.01 mmol to 61.88 mmol and from 10.23 mmol to 12.43 mmol, respectively. Mean
455 Mg and Ca content in seawater for each condition are summarized in **Table 3**. At the
456 rearing site level, comparison of ICP-OES results from the Paris and Roscoff control tanks

(P1 and R1) indicates that natural seawater contains, on average, approximately 4 mmol more Mg and 1.5 mmol less Ca than artificial seawater, resulting in a higher Mg/Ca ratio in NSW.

Between conditions, ICP-OES results reveal a gradual increase in Mg concentrations in artificial seawater from 51.01 ± 0.66 to 58.30 ± 1.32 mmol between conditions P1 and P3. Similarly, in natural seawater, Mg concentrations increase from 55.21 ± 0.21 to 61.88 mmol between R1 and R2, and from 55.21 ± 0.21 to 57.07 mmol between R1 and R3, indicating successful magnesium enrichment under the different rearing conditions. However, although the overall trend is consistent with expectations, the magnitude of the measured Mg differences between conditions do not always match the targeted enrichments. For instance, the Mg difference between conditions P1 and P2 (6 mmol) closely matchs the expectation (5.22 mmol) while the difference between P1 and P3 is limited to 7.2 mmol, thus, lower than the anticipated 10.44 mmol. This pattern is consistent with salinity measurements, which show no significant difference between P2 and P3. Similar discrepancies are observed under natural seawater conditions where Mg increase between R1 and R3 is limited to 1.86 mmol ± 0.66, again lower than the expected 5.22 mmol, while the Mg difference between R1 and R2 (6.67 mmol) closely match expectation.

On a weekly scale, daily monitoring of elemental concentrations in the ASW carried out at the Paris site reveals limited variations in Mg and Ca concentrations (< 1 mmol for Ca and 5 mmol for Mg) confirming that periodic water renewal effectively maintains target concentrations in each tank (**Supplement data 1, Figure S8**).

Finally, we note that salinity show no significant correlation with Mg/Ca ratios measured in ASW (**Supplementary data 1, Figure S9**) confirming the decoupling of these two parameters under experimental conditions.

4.3.2. Mg complexes in seawater.

Combined results from ICP-OES and ion chromatography (IC) carried out on seawater indicate that, even in the absence of EDTA, organic Mg complexes are present

in oyster rearing environment (**Table 3**). These organic Mg complexes were detected in both artificial seawater and natural seawater and represent a variable fraction of the total Mg, ranging from 0% (0 ± 0.8%) to 29 ± 5% (**Table 2**, **Figure 6**).

As illustrated in the Figure 6, the proportion of organic Mg complexed varies a lot between the different experimental conditions (**Figure 6**). For instance, conditions P1, P2, R1, and R2 contained substantial amounts of complexed Mg (ranging from 12% to 29%), whereas P3 and R4 showed little to no organic complexed Mg (**Table 2**). This variability seems to suggests that the formation and stability of organic Mg complexes are dependent on oyster rearing conditions.

The ICP OES and IC analyses conducted in this study do not allow us to identify the precise nature of the organic ligands involved in Mg complexation, which could have helped explain the observed differences in Mg organic complexes content between tanks. Nevertheless, a possible hypothesis is that the organically complexed Mg detected in aquarium seawater originates from oyster biological activity (e.g., degradation of oyster-derived organic matter) and/or from food-related inputs. Under this hypothesis, the large variability in the proportion of complexed Mg observed among experimental tanks (**Figure 6**) could arise from differences in oyster biological activity or from variations in the stability of organic ligands under the different experimental conditions.

4.3.3. Mg content of feed solutions

ICP-OES analysis reveals significant differences in Mg content between the solutions used for daily feeding of M. gigas. *Instant algae* contain approximately 4.6 mmol of Mg, whereas the Skeletonema solution contains 198 mmol of Mg, roughly 43 times higher than in Instant Algae. This observation is consistent with previous findings showing that diatoms tend to have higher Mg concentrations than other phytoplankton groups (Ho et al., 2003).

4.4. Mg/Ca in oyster shells

The range for all shell Mg/Ca (**Figure 7**) extends from 0.31 to 51.80 $mM.M^{-1}$, with a median value of 6.26 $mM.M^{-1}$ (mean = 7.56 $mM.M^{-1}$). Detailed descriptions of values are reported in **Table 4**. Shell Mg/Ca presents a gradual increase from P1 to P3 with increasing free Mg in seawater. Shell Mg/Ca are also higher in R2 compared to R1, following the same observation. We also note higher shell Mg/Ca in R3 with complexed Mg compared to R2 with free Mg in the same concentrations. Finally, diet change, R4, is reflected by an increased shell Mg/Ca compared to control.

5. Discussion

5.1. Influence of diet on shell Mg/Ca

The LA ICP-MS analyses carried out in this study reveal a shift of 3.8 $mmol.mol^{-1}$ in the Mg/Ca ratio of *M. gigas* shells following change in oyster's diet (**Figure 7**). Specifically, oysters exhibit a systematic increase in Mg/Ca after their diet was switched from Instant Algae to *Skeletonema* (**Figure 7, Table 2**) suggesting that diet plays a key role in modulating Mg incorporation into the shell.

Previous studies on bivalve diets have consistently shown that both food quantity and quality can significantly influence shell growth rates (e.g., Walne, 1976; Elsaesser, 2014). Because crystal growth rate has also been identified as a potentially important factor controlling elemental incorporation in abiogenic carbonates (e.g., Mucci and Morse et al, 1983; Lopez et al, 2009; Mavromatis et al, 2013, 2022) and biogenic carbonates (e.g., Vander Putten et al., 2000; Takesue & van Geen, 2004; Gillikin et al., 2005; Lorrain et al., 2005; Freitas et al., 2008; Schöne et al., 2011; Poulain et al., 2015, Tanaka et al, 2019), a first possible explanation for the higher shell Mg/Ca ratios observed under R4 compared to R1 conditions could be related to the increased shell growth rates observed between these two treatments (**Figure 5**). However, our results show that, at the individual scale, shell Mg/Ca values are not significantly correlated with growth rate under either R1 and R4 conditions (**Supplementary data 1, Figure S6**). Consequently, the observed increase in shell Mg/Ca from R1 to R4 can not be explained by growth-rate effects on Mg incorporation and instead indicate a direct influence of dietary source on magnesium incorporation into the shell. Although, to our knowledge, this effect has never been

549 documented in bivalves, experimental studies have shown a similar dietary control on
550 the Mg/Ca ratio of sea urchin tests. In particular, these studies have shown that the
551 Mg/Ca ratio of sea urchins is sensitive both to the type of diet (Asnaghi et al., 2014) and
552 to the Mg content of the food when the same diet is provided (Kolbulk et al., 2019, 2020).
553 In this study, we cannot unequivocally determine whether the observed variations in shell
554 Mg/Ca are primarily controlled by the Mg content of the diet or by differences in
555 digestion/assimilation efficiency between the two diets, or by a combination of these
556 factors. Addressing this question would require a dedicated experiment, in which the
557 same type of food would be provided to the oysters, with only one food artificially
558 enriched with Mg. Nevertheless, the consistency between our results and those obtained
559 for other calcifying organisms strongly suggests that the impact of diet on shell Mg/Ca is
560 primarily driven by the Mg content of the food itself.
561
562 These results highlight that food is a major source of Mg for oyster shell, and that diet
563 exerts a control on shell Mg/Ca. Failing to consider this effect may lead to inaccurate
564 reconstructions of seawater temperature based on shell Mg/Ca, with errors on
565 temperature estimated from 5.4°C to 14.4°C based on Mouchi et al. (2013) and Tynan et
566 al. (2017) respectively. Furthermore, open marine settings constitute a substantially
567 larger reservoir than estuarine systems and are likely less influenced by pronounced
568 seasonal fluctuations relative to estuarine environment. As a result, nutrient
569 concentrations can be expected to exhibit greater variability within estuarine settings
570 than in open marine settings. This implies that bias on temperature reconstruction due
571 to changes in food source should be substantially more pronounced in estuarine settings
572 compared to open marine settings. Therefore, food source variability probably
573 contributes to the divergence between environmental settings in Mg/Ca–T models
574 (**Figure 8**).

575 **5.2. Influence of Mg form and Mg/Ca of seawater on shell Mg/Ca**

576 ***5.2.1. Complexed Mg in seawater remains bioavailable for oyster shell***
577 ***incorporation***

578 The rearing experiment performed with natural seawater aimed at assessing the
579 bioavailability of Mg when trapped in molecules with covalent bonds. Our results indicate

that a higher concentration in seawater of identical proportions of free (R2 tank) and complexed Mg (R3 tank) induces an increased uptake of Mg in oyster shells compared to control conditions (R1 tank; **Figure 7**). Notably, shell Mg/Ca ratios increased by 7.04 in R3 while only of 2.68 in R2 relative to R1 (**Table 3**). This demonstrates that even when Mg is bound to strong organic chelators, such as EDTA, oysters can break these chemical bonds and access the Mg for metabolic processes and shell incorporation. This suggest that in natural settings, Mg uptake in shells is equivalent whether Mg is released from organic ligands or directly available in free form. Therefore, the Mg form in seawater does not explain the variety of shell Mg/Ca values found in the literature (in oysters: Surge & Lohmann, 2008; Mouchi et al., 2013; Tynan et al., 2017; in other bivalves: Wanamaker et al., 2008; Schleinkofer et al., 2021; Mouchi et al., 2025b).

The mechanism by wich Mg-EDTA bound are broken to allow incorporation of Mg in the shell could also explain the strong mortality observed in R3. The commercial Mg-EDTA used (TCI, ref. E0094) was chosen as it was stable when put in solution in deionized water, and exhibited a pH of 8 (*i.e.*, compatible with oyster rearing). However, when oysters dissociate Mg from EDTA, the liberated EDTA enters the tissues in its free form, where it can chelate other trace metals, probably necessary for their metabolism. Many of these chemical elements are cofactors to enzymatic processes (*e.g.*, Zn for carbonic anhydrase; Lee et al., 1995) or included in metal-binding proteins (*e.g.*, Cu and Cd; Imber et al., 1987; Motekaitis and Martell, 1987). The pronounced increase in Mg/Ca observed in shell from R3 may also be related to the poor physiological condition of oysters. Indeed, the degradation of oyster health, may have impaired the biological regulation of element incorporation during shell formation, leading to a less controlled uptake of trace elements such as Mg.

5.2.2. Higher concentration of Mg in seawater increases shell Mg/Ca

Results from Mg-enriched seawater experiments (P1, P2, P3, R1, R2) provide clear evidence that seawater Mg concentration exerts a strong control on shell Mg/Ca. At both rearing sites, and regardless of seawater type, we observed an increase in shell Mg/Ca with increased Mg concentration in seawater (**Figure 7, Table 3**). Similar positive

relationships between Mg/Ca ratio in the shell and seawater Mg/Ca have also been documented in other biogenic carbonates such as foraminifera (Segev and Erez, 2006; Mewes et al, 2014, De Nooijer et al, 2017). This result suggests that the incorporation of Mg in oyster shell is at least partly controlled by ambient seawater Mg concentration.

In artificial seawater, where three levels of Mg enrichment were tested (tanks P1, P2, P3), a positive linear relationship was observed between shell Mg/Ca and seawater Mg/Ca (**Figure 8b**). This relationship is described by the following equation:

Mg/Ca_{shell} ($mmol.mol^{-1}$) = 0.0029 (± 0.0005) × $Mg/Ca_{seawater}$ + (-5.4612 ± 2.0739), ($r^2 \approx$ 0.992)

A comparable increase in shell Mg/Ca with increasing seawater Mg/Ca ratio was observed for oysters reared in natural seawater (tanks R1 & R2, **Figure 7**). However, only two levels of Mg enrichment were tested under natural seawater conditions, which prevents the adjustment of a linear model. Despite this limitation, it is worth noting that Mg/Ca in shell increases with Mg/Ca ratio both in natural seawater and in artificial seawater experiments (**Figure 8b**). This similarity suggests that the mechanism promoting Mg incorporation in the shell associated with increasing seawater Mg concentration is the same regardless of seawater type.

On the other hand, one could also notice that for a given seawater Mg/Ca, shell Mg/Ca values systematically differ between oysters reared in natural and artificial seawater (**Figure 8b**). Specifically, for approximately the same seawater Mg/Ca ratio (5200 mmol/mol) oysters grown in artificial seawater exhibit significantly higher shell Mg/Ca (+ 3.72 mmol/mol) than those grown in natural seawater (**Table 3**). Because shell growth rates do not differ substantially between these conditions (**Figure 5**), this offset cannot be attributed to growth-rate effects. Instead, this difference likely reflects variations in seawater composition beyond Mg and Ca concentrations alone. Indeed, artificial seawater may differ from natural seawater in terms of alkalinity and pH, two parameters that were also shown to influence Mg partitioning in calcite (e.g., Russel et al, 2004; Alvarez Caraveo et al, 2025). An alternative explanation may relate to differences in the experimental setup, as oysters were not reared under strictly identical conditions

641 at Paris (artificial seawater) and Roscoff (natural seawater) (**Figure 2**). At Paris, oysters
642 were maintained in smaller aquaria with more frequent water renewal, whereas in
643 Roscoff oyster were reared in larger aquaria and the water renewal setup was designed
644 to minimize disturbance of the organisms. The experimental conditions in Paris may
645 therefore have imposed a higher level of physiological stress to the oyster. Although this
646 stress did not markedly affect shell growth rates, it may have disrupted biological
647 processes controlling elemental incorporation, potentially leading to enhanced Mg
648 incorporation in the shell.

649 ***5.2.3. Impact of seawater Mg/Ca on reconstructed temperatures***

650 Numerous relationships between Mg/Ca and temperature in oysters and mussels
651 have been reported in the literature (Mouchi et al., 2018). At the same temperature,
652 reported Mg/Ca values vary substantially across species and localities. For example, over
653 the range of 0 to 25°C, Mg/Ca ratios vary from 1 to 6 $mmol.mol^{-1}$ in *M. gigas* from France
654 (Mouchi et al., 2013), from 10 to 20 $mmol.mol^{-1}$ in *Mytilus edulis* reared in aquarium
655 (Wanamaker et al., 2008), and from 10 to 40 $mmol.mol^{-1}$ in *Acesta excavata* collected
656 from deep-sea Norwegian Atlantic region; Schleinkofer et al., 2021).
657
658 Among published Mg/Ca-T calibrations in bivalves, the model of Freitas et al.
659 (2008) provides the closest estimate to measured temperature (19.0°C) for oysters
660 reared in artificial seawater under control conditions (P1), with a reconstructed
661 temperature of 20.8°C (**Supplementary data 1, Table S4**). In contrast, the most accurate
662 model for the oyster reared in control conditions in natural seawater (R1) is the one of
663 Mouchi et al. (2013), which reconstruct 23.4°C. This discrepancy is likely due to the
664 contrasted seawater Mg/Ca between NSW and ASW (**Table 2**). Considering the
665 calibration of Freitas et al. (2008) Mg^{2+} enrichment in ASW in P2 and P3 induces
666 overestimations of seawater temperature of 3.2°C and 9.2°C, respectively. In the NSW
667 experiment, Mg^{2+} enrichment of 6.67 mmol (R2) corresponds to an apparent temperature
668 overestimation of 10.1°C, whereas the complexed Mg enrichment (R3) result in a
669 substantially larger overestimation of +26.6°C (**Supplementary data 1, Table S4**). The
670 poor health condition of oysters from R3 is probably responsible of at least part of that
671 important increase, as the EDTA released in their body has most probably negatively

672 impacted a variety of metabolic biochemical processes. At this stage it is impossible to
673 determine the extent of those impacts and the resulting changes in the chemistry of the
674 extrapallial-fluid (EPF) from which shell precipitates. In particular, this can influence the
675 pH and calcium saturation index of the EPF which have been reported to impact Mg/Ca
676 in carbonates (e.g., Kisakürek et al., 2008; Mavromatis et al., 2017; Gray and Evans, 2019;
677 Alvarez Caraveo et al., 2025, **Figure 8a**), although other studies reported no significant
678 impact of pH on shell Mg/Ca (e.g., Davis et al., 2017).
679
680 Based on both these experiments (NSW and ASW), we can assert that seawater
681 Mg/Ca has a substantial impact on shell Mg/Ca (**Figure 8b**), and therefore on
682 reconstructed temperatures from shell Mg/Ca.
683
684 The same conclusion was previously made by Tynan et al. (2017), although the
685 difference observed by the authors on seawater Mg/Ca between their two study areas
686 was relatively low (between 5300 $mmol.mol^{-1}$ and 5600 $mmol.mol^{-1}$– with one short drop
687 at 4600 $mmol.mol^{-1}$, and stable around 5600 $mmol.mol^{-1}$ at Pambula Lake and Moreton
688 Bay, respectively). In our experiments, seawater Mg/Ca ranged from 4233 $mmol.mol^{-1}$to
689 5821 $mmol.mol^{-1}$(**Table 2**), and this relatively narrow range already produces substantial
690 changes in shell Mg/Ca (i.e., an increase of up to +2.42 $mmol.mol^{-1}$).
691
692 Recently, Lebrato et al. (2020) compiled measurements of modern seawater
693 Mg/Ca ratios taken all around the world. Their data indicate that the Mg/Ca ratio of current
694 seawater in the open marine environment fluctuates between 4900 and 5300 $mmol.mol^{-1}$, whereas environments influenced by riverine inputs exhibit greater variability, with
696 Mg/Ca ratios ranging approximately from 4400 to 6400 $mmol.mol^{-1}$. Based on the
697 correlation between shell Mg/Ca and seawater Mg/Ca we observed in this study (**Figure**
698 **8b**), such natural variability in seawater Mg/Ca could induce changes in shell Mg/Ca
699 exceeding 1.2 $mmol.mol^{-1}$ for shells originating from open-marine environments and 6
700 $mmol.mol^{-1}$ for shells from estuarine environments. Such seawater-driven variations in
701 shell Mg/Ca could translate into temperature reconstruction errors exceeding 8–22 °C if
702 not accounted for in Mg/Ca-T calibrations.
703

Thus, the dependence of shell Mg/Ca on seawater magnesium content together with natural variability in seawater Mg/Ca, may contribute to the discrepancies among published Mg/Ca–T calibrations. However, assessing the influence of seawater composition on previously published Mg/Ca–temperature relationships remain challenging, as only a limited number of studies report seawater Mg/Ca values alongside shell Mg/Ca ratios (e.g., Surge & Lohmann, 2008; Tynan et al., 2017). Future studies should therefore systematically report seawater Mg/Ca to allow a more precise evaluation of its impact on Mg/Ca-based temperature reconstructions.

5.3. Potential factors explaining the discrepancies between Mg/Ca-temperature models and implications on temperature reconstructions

The **figure 8a** summarizes the environmental and endogenous factors known to affect shell Mg/Ca. Although previous studies demonstrated the influence of temperature and some endogenous ("vital effects") on Mg incorporation in bivalve shells (e.g., Gillikin et al., 2005; Lazareth et al., 2007; Schöne et al., 2011, 2013; Mouchi et al., 2013; Alvarez Caraveo et al., 2025), these mechanisms alone cannot explain discrepancies observed between Mg/Ca-temperature models derived from marine and estuarine environments (**Figure 1**). The results of this study clearly indicate the influence of additional environmental parameters on shells Mg/Ca. Notably, we found that both seawater Mg/Ca and food source can markedly affect shell Mg/Ca (**Figure 8c**). Those could be responsible for environmental specific Mg/Ca-T models.

As we demonstrated, shell Mg/Ca increases with seawater Mg/Ca. Therefore, for similar environmental settings, we can assume that seawater Mg/Ca primarily controls the models y-intercepts (Tynan et al., 2017, **Figure 8b**). On the other hand, the sensibility of Mg/Ca to temperature (specific to marine and estuarine environments) should be governed by other factors. In particular, we need to identify a seasonal environmental parameter whose expression is accentuated during summer in estuarine environments. Based on our results, a potential candidate would be a change in the relative contribution of food sources between marine and continental origins with distinct Mg/Ca ratios. A

similar interpretation has been proposed to explain differences in $\delta^{13}C$ values of bivalve shells between marine and estuarine settings (Milano et al., 2019; Mouchi et al., 2020).

Overall, estuarine environments are characterized by greater variability in both water (Lebrato et al, 2020) and food sources (e.g., O'Boyle and Silke, 2010), resulting in more complex shell Mg/Ca signals than marine settings. Reconstruction of temperature using Mg/Ca-based temperature reconstructions from open marine bivalve shells should be less biased, as external conditions are more stable. Alternatively, in estuarine settings, shell Mg/Ca records contain additional environmental information that can be deconvoluted to improve our knowledge on past coastal water composition and ecosystem dynamics.

6. Conclusion

In this study, we conducted controlled culture experiments to investigate the influence of both form and source of Mg on bivalve shell Mg/Ca ratio. Our results confirm that magnesium is present in natural seawater not only as free ions but also as complexes with organic ligand. Mg remains bioavailable to oysters even when complexed with strong organic ligands such as EDTA. Our results further suggest that Mg form in seawater has no influence on shells Mg/Ca. In contrast shell Mg/Ca strongly co-varies with seawater Mg/Ca and food source, with a potential positive correlation between dietary Mg/Ca and the Mg/Ca recorded in shells.

Based on these results, we recommend that further aquarium experiments and in situ calibration studies explicitly consider both seawater Mg/Ca and food Mg/Ca when developing Mg/Ca-temperature models. Moreover, paleoenvironmental reconstructions based on Mg/Ca should choose appropriate models regarding the environmental settings of studied fossils.

Acknowledgements:

This study was funded by the INSU TelluS INVISITE project. M.P. was funded by the Master grant from the Institut de l'Océan, Alliance Sorbonne Université. V.M. was funded by the ANR CERBERUS project (ANR-17-CE02-0003). We are grateful to the editor, V.

765 Mavromatis, and to the two anonymous reviewers, who provided helpful comments and
766 suggestions that greatly improved the original manuscript.
767

768 **Data Availability:**

769 The Mg/Ca ratio measured by LA-IPC-MS on oyster shells are accessible at:
770 10.5281/zenodo.17552463
771 All the over research data supporting this work including, rearing experiment monitoring,
772 ICP-OES and Ion chromatography results been provided as supplementary data.
773

774 **Supplementary Material:**

775 The following files are the Supplematerial Material to this article.
776 **Supplementary Data 1** is a Word document summarizing (1) oyster shell labeling, (2)
777 seawater physicochemical monitoring and associated statistical test results, (3) growth
778 rate and mortality data, (5) comparison between shell Mg/Ca measured in different
779 laboratories, (6) effect of seawater renewal on Mg concentration in seawater and (7)
780 comparison between reconstructed temperature from shell Mg/Ca based on different
781 model published in the literature. **Supplementary Data 2** is an Excel file containing daily
782 monitoring of temperature, salinity, and oyster mortality grown in artificial seawater. The
783 dates on which oyster were marked with Mn^{2+} are also indicated. **Supplementary Data**
784 **3** is an Excel file with daily temperature in natural seawater. The dates on which oyster
785 were marked with Mn^{2+} are also indicated. **Supplementary Data 4** summarize ICP-OES
786 results obtained on weekly sampled seawater samples in artificial seawater before and
787 after water renewal. **Supplementary Data 5** correspond to complete ICP-OES results of
788 measured artificial and natural seawater samples as well as oyster feeding solution.
789 **Supplementary Data 6** correspond to Ion chromatography results.
790

791 **References:**

792 Alvarez Caraveo, B., Guillermic, M., Downey-Wall, A., Cameron, L.P., Sutton, J.N.,
793 Higgins, J.A., Ries, J.B., Lotterhos, K., Eagle, R.A., 2025. Magnesium
794 (Mg/Ca, δ^{26}Mg), boron (B/Ca, δ^{11}B), and calcium (Ca^{2+}) geochemistry of *Arctica*

islandica and *Crassostrea virginica* extrapallial fluid and shell under ocean acidification. Biogeoscience 22, 12, 2831-2851.

Asnaghi, V., Mangialajo, L., Gattuso, J. P., Francour, P., Privitera, D., & Chiantore, M., 2014. Effects of ocean acidification and diet on thickness and carbonate elemental composition of the test of juvenile sea urchins. Marine environmental research, 93, 78-84.

Bougeois, L., de Rafélis, M., Reichart, G.-J., de Nooijer, L.J., Dupont-Nivet, G., 2016. Mg/Ca in fossil oyster shells as palaeotemperature proxy, an example from the Palaeogene of Central Asia. Palaeogeogr. Palaeoclimatol. Palaeoecol. 441, 611–626.

Briard, J., Pucéat, E., Vennin, E., Daëron, M., Chavagnac, V., Jaillet, R., Merle, D., de Rafélis, M., 2020. Seawater paleotemperature and paleosalinity evolution in neritic environments of the Mediterranean Margin: insights from isotope analysis of bivalve shells. Palaeogeogr. Palaeoclimatol. Palaeoecol. 543, 109582.

Chauvaud, L., Lorrain, A., Dunbar, R.B., Paulet, Y-M., Thouzeau, G., Jean, F., Guarini, J-M., Mucciarone, D., 2005. Shell of the Great Scallop *Pecten maximus* as a high-frequency archive of paleoenvironmental changes. Geochem. Geophy. Geosyst. 6.

Chipman, W. A. 1966. Uptake and accumulation of chromium-51 by the clam, Tapes decussatus, in relation to physical and chemical form. In Disposal of Radioactive Wastes into Seas, Oceans and Surface Waters, Proc. Symp., Vienna, 16-20 May 1966, 571- 82. IAEA, Vienna, 898.

Chumanov, R.S. and Burgess, R.R., 2011. Artifact-inducing enrichment of ethylenediaminetetraacetic acid and ethyleneglycoltetraacetic acid on anion exchange resins. Anal biochem 412, 1, 34-39.

Davis, C.V., Fehrenbacher, J.S., Hill, T.M., Russell, A.D., Spero, H.J., 2017. Relationships between temperature, pH, and crusting on Mg/Ca ratios in laboratory-grown *Neogloboquadrina* foraminifera. Paleoceanogr. 32, 1137–1152.

Dyrssen, D., and Wedborg, M. 1974. Equilibrium calculations of the speciation of elements in sea water. The sea 5, 181-195.

825 Elsaesser, W.N. 2014. Influence of diet on element incorporation in the shells of two
826 bivalve molluscs: *Argopecten irradians concentricus* and *Mercenaria mercenaria*.
827 PhD dissertation, University of South Florida.
828 Epstein, S., Buchsbaum, R., Lowenstam, H.A. and Urey, H.C., 1953. Revised carbonate-
829 water isotopic temperature scale. Geological Society of America Bulletin, 64,
830 1315-1326.
831 Freitas, P., Clarke, L., Kennedy, H., Richardson, C., 2008. Inter-and intra-specimen
832 variability masks reliable temperature control on shell Mg/Ca ratios in laboratory
833 and field cultured *Mytilus edulis* and *Pecten maximus* (Bivalvia). Biogeoscience
834 Discussions 5, 1245-1258.
835 Gillikin, D.P., Lorrain, A., Navez, J., Taylor, J.W., André, L., Keppens, E., Baeyens, W.,
836 Dehairs F., 2005. Strong biological controls on Sr/Ca ratios in aragonitic marine
837 bivalve shells. Geochem. Geophys. Geosyst. 6, Q05009.
838 Gray, W. R., Evans, D., 2019. Nonthermal influences on Mg/Ca in planktonic foraminifera:
839 a review of culture studies and application to the Last Glacial Maximum.
840 Paleoceanogr. Paleoclimatol. 34, 306–315.
841 Hausmann, N., Siozos, P., Lemonis, A., Colonese, A.C., Robson, H.K., Anglos, D., 2017.
842 Elemental mapping of Mg/Ca intensity ratios in marine mollusc shells using Laser-
843 Induced Breakdown Spectroscopy. J. Anal. At. Spectrom. 32, 8, 1467–1472.
844 Hirose, K. 2006. Chemical speciation of trace metals in seawater: a review. *Anal. Sci* 22,
845 1055-1063.
846 Ho, T.-Y., Quigg, A., Finkel, Z.V., Milligan, A.J., Wyman, K., Falkowski, P.G., Morel, F.M.M.,
847 2003. The elemental composition of some marine phytoplankton. J. Phycol. 39, 6,
848 1145-1159.
849 Hunter, K.A., Boyd, P.W., 2007. Iron-binding ligands and their role in the ocean
850 biogeochemistry of iron. Environ. Chem. 4, 4, 221-232.
851 Huyghe, D., Lartaud, F., Emmanuel, L., Merle, D., Renard, M., 2015. Palaeogene climate
852 evolution in the Paris Basin from oxygen stable isotope ($\delta^{18}O$) compositions of
853 marine molluscs. J. Geol. Soc. 172, 5, 576–587.
854 Huyghe, D., de Rafélis, M., Ropert, M., Mouchi, V., Emmanuel, L., Renard, M., Lartaud, F.,
855 2019. New insight into oyster high-resolution shell growth patterns. Marine Biology
856 166, 48.

Imber, B.E., Thompson, J.A.J., Ward, S., 1987. Metal-binding protein in the Pacific Oyster, *Crassostrea gigas*: assessment of the protein as a biochemical environmental indicator. Bull Environ Contam and Toxicol 38, 707-714.

Jochum, K.P., Nohl, U., Herwig, K., Lammel, E., Stoll, B., Hofmann, A.W., 2005. GeoReM: a new Geochemical Database for Reference Materials and isotopic standards. Geostand. Geoanal. Res. 29, 333–338.

Kirby, M. X., Soniat, T. M. and Spero, H. J. 1998. Stable isotope sclerochronology of Pleistocene and recent oyster shells (*Crassostrea virginica*). Palaios 13, 560–569.

Kısakürek, B., Eisenhauer, A., Böhm, F., Garbe-Schönberg, D., Erez, J., 2008. Controls on shell Mg/Ca and Sr/Ca in cultured planktonic foraminiferan, *Globigerinoides ruber* (white). Earth Planet. Sci. Lett. 273, 3–4, 260-269.

Klein, R.T., Lohmann, K.C., Thayer, C.W, 1996. Bivalve skeletons record sea-surface temperature and $\delta^{18}O$ via Mg/Ca and $^{18}O/^{16}O$ ratios. Geology 24, 415–418.

Kołbuk, D., Dubois, P., Stolarski, J., & Gorzelak, P., 2019. Effects of seawater chemistry (Mg2+/Ca2+ ratio) and diet on the skeletal Mg/Ca ratio in the common sea urchin Paracentrotus lividus. Marine environmental research, 145, 22-26.

Kołbuk, D., Di Giglio, S., M'Zoudi, S., Dubois, P., Stolarski, J., & Gorzelak, P., 2020. Effects of seawater Mg2+/Ca2+ ratio and diet on the biomineralization and growth of sea urchins and the relevance of fossil echinoderms to paleoenvironmental reconstructions. Geobiology, 18(6), 710-724.

Langlet, D., Alunno-Bruscia, M., Rafélis, M.D., Renard, M., Roux, M., Schein, E. and Buestel, D., 2006. Experimental and natural cathodoluminescence in the shell of Crassostrea gigas from Thau lagoon (France): ecological and environmental implications. Mar. Ecol. Prog. Ser. 317, 143-156.

Lartaud, F., de Rafelis, M., Ropert, M., Emmanuel, L., Geairon, P. and Renard, M., 2010. Mn labelling of living oysters: artificial and natural cathodoluminescence analyses as a tool for age and growth rate determination of *C. gigas* (Thunberg, 1793) shells. Aquaculture 300, 1-4, 206-217.

Lartaud, F., Emmanuel, L., De Rafélis, M., Ropert, M., Labourdette, N., Richardson, C. A., Renard, M. 2010. A latitudinal gradient of seasonal temperature variation recorded in oyster shells from the coastal waters of France and The Netherlands. Facies 56, 13-25.

889 Lazareth, C.E., Guzman, N., Poitrasson, F., Candaudap, F., Ortlieb, 2007. Nyctemeral
890 variations of magnesium intake in the calcitic layer of a Chilean mollusk shell
891 (*Concholepas concholepas*, Gastropoda). GCA 71, 5369-5383.
892 Le Corre, P., Tréguer, P., Courtot, P. 1972. Evaluation de matière organique dissoute dans
893 des eaux côtières de la Bretagne méridionale en avril 1970. Cahier de Biologie
894 Marine 13, 443-455
895 Lebrato, M., Garbe-Schönberg, D., Müller, M. N., Blanco-Ameijeiras, S., Feely, R. A.,
896 Lorenzoni, L., ... & Oschlies, A., 2020. Global variability in seawater Mg: Ca and Sr:
897 Ca ratios in the modern ocean. Proceedings of the National Academy of Sciences,
898 117(36), 22281-22292.
899 Lee, J., Morel, F., 1995. Replacement of zinc by cadmium in marine phytoplankton. Mar.
900 Ecol. Prog. Ser. 127, 305–309.
901 Longerich, H.P., Jackson, S.E., Günther, D., 1996. Inter-laboratory note. Laser ablation
902 inductively coupled plasma mass spectrometric transient signal data acquisition
903 and analyte concentration calculation. J. Anal. At. Spectrom. 11, 899-904.
904 Lopez, O., Zuddas, P., & Faivre, D., 2009. The influence of temperature and seawater
905 composition on calcite crystal growth mechanisms and kinetics: Implications for
906 Mg incorporation in calcite lattice. Geochimica et Cosmochimica Acta, 73(2), 337-
907 347.
908 Lorrain, A., Gillikin, D.P., Paulet, Y.M., Chauvaud, L., Le Mercier, A., Navez, J., Andreì, L.
909 2005. Strong kinetic effects on Sr/Ca ratios in the calcitic bivalve *Pecten*
910 *maximus*. Geology 33, 12, 965–968.
911 Marchand, M. 1974. Considérations sur les formes physico-chimiques du cobalt,
912 manganèse, zinc, chrome et fer dans l'eau de mer enrichie ou non en matière
913 organique. *J. Cons. Int. Explor. Mer* 35, 2, 130-142.
914 Mavromatis, V., Gautier, Q., Bosc, O., & Schott, J. (2013). Kinetics of Mg partition and Mg
915 stable isotope fractionation during its incorporation in calcite. Geochimica et
916 Cosmochimica Acta, 114, 188-203.
917 Mavromatis, V., Immenhauser, A., Buhl, D., Purgstaller, B., Baldermann, A., Dietzel, M.,
918 2017. Effect of organic ligands on Mg partitioning and Mg isotope fractionation
919 during low-temperature precipitation of calcite in the absence of growth rate
920 effects. Geochim. Cosmochim. Acta 207, 139-153.

Mavromatis, V., Brazier, J. M., & Goetschl, K. E. (2022). Controls of temperature and mineral growth rate on Mg incorporation in aragonite. Geochimica et Cosmochimica Acta, *317*, 53-64.

Mewes, A., Langer, G., De Nooijer, L. J., Bijma, J., & Reichart, G. J. 2014. Effect of different seawater Mg2+ concentrations on calcification in two benthic foraminifers. Marine micropaleontology, *113*, 56-64.

Milano, S., Schöne, B.R., Gutierrez-Zugasti, I., 2019. Oxygen and carbon stable isotopes of *Mytilus galloprovincialis* Lamarck, 1819 shells as environmental and provenance proxies. The Holocene, 30, 65-76.

Motekaitis, R.J., Martell, A.E., 1987. Speciation of metals in the oceans. I. Inorganic complexes in seawater, and influence of added chelating agents. Mar. Chem. 21, 2, 101-116.

Mouchi, V., de Rafélis, M., Lartaud, F., Fialin, M., Verrecchia E., 2013. Chemical labelling of oyster shells used for time-calibrated high resolution Mg/Ca ratios: a tool for past estimation of seasonal temperature variations. Palaeogeogr. Palaeoclimatol. Palaeoecol. 373, pp. 66-74.

Mouchi, V., Briard, J., Gaillot, S., Argant, T., Forest, V., Emmanuel, L., 2018. Reconstructing environments of collection site from archaeological bivalve shells: case study from oysters (Lyon, France). J. Archaeol. Sci. Rep., 21, 1225-1235.

Mouchi, V., Emmanuel, L., Forest, V., Rivalan, A., 2020. Geochemistry of bivalve shells as indicator of shore position of the 2nd c. BC. Open Quat. 6, 4, 1-15.

Mouchi, V., Andrus, C.F.T., Checa, A.G., Elliot, M., Griesshaber, E., Hausmann, N., Huyghe, D., Lartaud, F., Peharda, M., de Winter, N.J., 2025. Oyster shells as archives of present and past environmental variability and life history traits: A multi-disciplinary review of sclerochronology methods and applications. L&O Letters 10, 179-199.

Mouchi, V., Nedoncelle, K., Bruguier, O., Le Bris, N., Garmirian, Z., Lartaud, F., 2025. Mg/Ca from mussel shells rather than $\delta^{18}O$ as a promising temperature proxy for hydrothermal vent ecosystems. Deep-Sea Res. I: Oceanogr. Res. Pap. 219, 104485.

Mucci, A., & Morse, J. W. 1983. The incorporation of Mg2+ and Sr2+ into calcite overgrowths: influences of growth rate and solution composition. Geochimica et Cosmochimica Acta, 47(2), 217-233.

De Nooijer, L. J., Van Dijk, I., Toyofuku, T., & Reichart, G. J. (2017). The impacts of seawater Mg/Ca and temperature on element incorporation in benthic foraminiferal calcite. Geochemistry, Geophysics, Geosystems, 18(10), 3617-3630.

O'Boyle, S., & Silke, J., 2010. A review of phytoplankton ecology in estuarine and coastal waters around Ireland. Journal of plankton research, 32(1), 99-118.

Pierre, C., 1999. The oxygen and carbon isotope distribution in the Mediterranean water masses. Mar. Geol. 153, 41-55.

Pouil, S., Metian, M., Dupuy, C., Teyssié, J.L., Warmau, M., Bustamante, P. 2020. Diet variably affects the trophic transfer of trace elements in the oyster *Crassostrea gigas*. Mar. Environ. Res. 161, 105124.

Poulain, C. Gillikin, D.P., Thébault, J., Munaron, J.M., Bohn, M., Robert, R., Paulet, Y.-M., Lorrain, A., 2015. Chem. Geol. 396, 42-50.

Purton L. and Brasier M. 1997. Gastropod carbonate $\delta^{18}O$ and $\delta^{13}C$ values record strong seasonal productivity and stratification shifts during the late Eocene in England. Geology 25, 10,871–874.

Rohling, E.J., 2000. Paleosalinity: confidence limits and future applications. Mar. Geol. 163, 1–11.

Russell, A. D., Hönisch, B., Spero, H. J., & Lea, D. W., 2004. Effects of seawater carbonate ion concentration and temperature on shell U, Mg, and Sr in cultured planktonic foraminifera. *Geochimica et Cosmochimica Acta*, *68*(21), 4347-4361.

Schleinkofer, N., Raddatz, J., Evans, D., Gerdes, A., Flögel, S., Voigt S., Büscher, J.V., Wisshak, M., 2021. Compositional variability of Mg/Ca, Sr/Ca, and Na/Ca in the deep-sea bivalve *Acesta excavata* (Fabricius, 1779). PLoS ONE, 16, e0245605.

Schöne, B.R., Gillikin, D.P., 2013. Unraveling environmental histories from skeletal diaries — advances in sclerochronology. Palaeogeogr. Palaeoclimatol. Palaeoecol. 373, 1–5.

Schöne, B. R., Zhang, Z., Radermacher, P., Thébault, J., Jacob, D. E., Nunn, E. V. & Maurer, A.-F., 2011. Sr/Ca and Mg/Ca ratios of ontogenetically old, long-lived bivalve shells (*Arctica*

islandica) and their function as paleotemperature proxies. *Palaeogeogr, Palaeoclimat, Palaeoecol* 302, 52–64.

Schöne, B.R., Radermacher, P., Zhang, Z., Jacob, D.E. 2013. Crystal fabrics and element impurities (Sr/Ca, Mg/Ca and Ba/Ca) in shells of *Arctica islandica* – Implication for paleoclimate reconstructions. Palaeogeogr. Palaeoclimatol. Palaeoecol. 373, 50-59.

Segev, E., & Erez, J. 2006. Effect of Mg/Ca ratio in seawater on shell composition in shallow benthic foraminifera. Geochemistry, Geophysics, Geosystems, *7*(2).

Shaked, Y., Lis, H., 2012. Disassembling iron availability to phytoplancton. Front. Microbiol. 3, 123.

Sharpe, J.C., London, E., 1997. Inadvertent concentrating of EDTA by ion exchange chromatography: avoiding artifacts that can interfere with protein purification. Anal. Biochem. 250, 124-125.

Surge, D., Lohmann, K.C., 2008. Evaluating Mg/Ca ratios as a temperature proxy in the estuarine oyster, *Crassostrea virginica*. J. Geophys. Res. 113, G02001.

Takesue, R.K., Van Geen, A., 2004. Mg/Ca, Sr/Ca, and stable isotopes in modern and holocene *Protothaca staminea* shells from a northern California coastal upwelling region. Geochim. Cosmochim. Acta, 68, 3845–3861.

Tanaka, K., Okaniwa, N., Miyaji, T., Murakami-Sugihara, N., Zhao, L., Tanabe, K., ... & Shirai, K. 2019. Microscale magnesium distribution in shell of the Mediterranean mussel Mytilus galloprovincialis: An example of multiple factors controlling Mg/Ca in biogenic calcite. Chemical Geology, 511, 521-532.

Tynan, S., Opdyke, B.N., Walczak, M., Eggins, S., Dutton, A. 2017. Assessment of Mg/Ca in *Saccostrea glomerata* (the Sydney rock oyster) shell as a potential temperature record. Palaeogeogr. Palaeoclimatol. Palaeoecol. 484, 79-88.

Urey, H.C., Lowenstam, H.A., Esptein, S., McKinney, C.R., 1951. Measurement of paleotemperatures and temperatures of the Upper Cretaceous of England, Denmark, and the Southeastern United States. GSA Bulletin 62, 4, 399-416.

Uvanovic, H., Schöne, B.R., Markulin, K., Janekovic, I., Peharda, M., 2021. Venerid bivalve *Venus verrucosa* as a high-resolution archive of seawater temperature in the Mediterranean Sea. Palaeogeogr. Palaeoclimatol. Palaeoecol. 561, 110057.

Vander Putten, E., Dehairs, F., Keppens, E., Baeyens, W., 2000. High resolution distribution of trace elements in the calcite shell layer of modern *Mytilus edulis*: environmental and biological controls. Geochim. Cosmochim. Acta, 64, 6, 997-1011.

Wafar, M., Le Corre, P., 1982, Evolution saisonnière de la matière organique dissoute dans les eaux côtières de la Manche Occidentale (Baie de Morlaix): Evolution simultanée du Carbone, de l'Azote et du Phosphore organique dissous. CNEXO Actes Colloq., 14, 47-66.

Walne, P.R., 1976. Experiments on the culture in the sea of the Butterfish Venerupis decussata L. Aquaculture, 8, 371-381.

Wanamaker, A.D., Kreutz, K.J., Wilson, T., Borns Jr. H.W., Introne, D.S., Feindel, S. 2008. Experimentally determined Mg/Ca and Sr/Ca ratios in juvenile bivalve calcite for *Mytilus edulis*: implications for paleotemperature reconstructions. Geo-Mar. Lett. 28, 359-368.

Wefer, G., Berger, W.H., 1991. Isotope paleontology: growth and composition of extant calcareous species. Mar. Geol. 100, 207-248.

WMO, 2025. https://wmo.int/topics/climate, World Meteorological Organization website, consulted on 05/21/25.

Zhang, J., Kattner, G., Koch, B.P., 2019. Interaction of trace elements and organic ligands in seawater and implications for quantifying biogeochemical dynamics: A review. Earth-Sci. Rev. 192, 631-649.

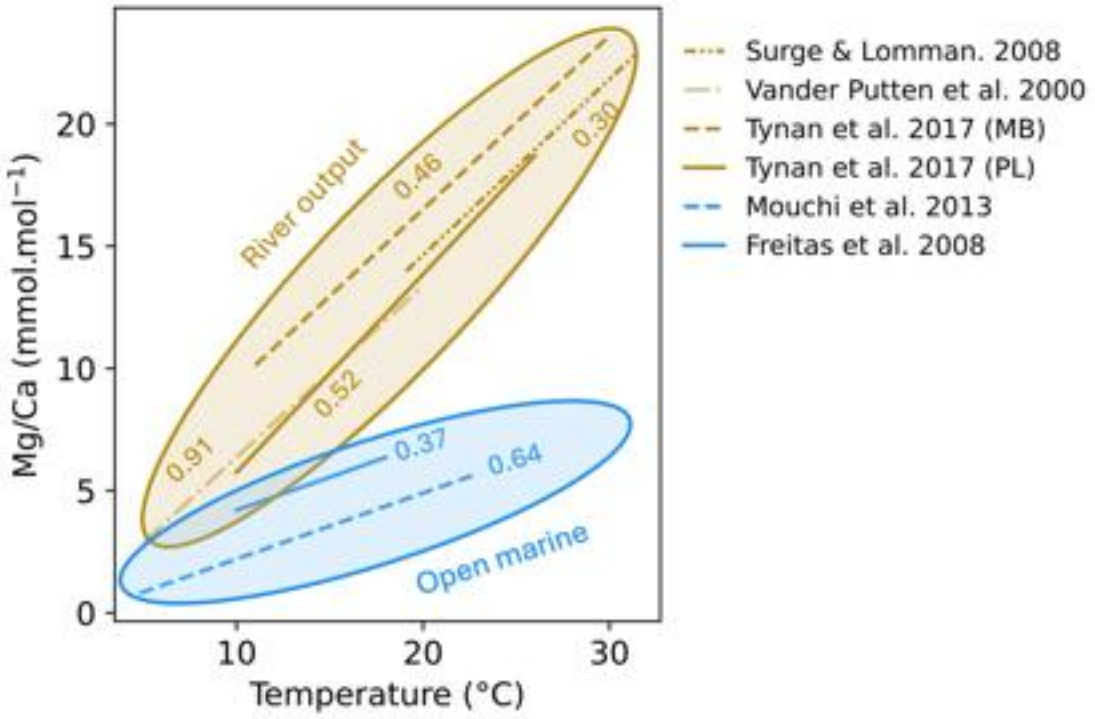

Figure 1: Existing calibrations of Mg/Ca in calcitic bivalve shell relative to seawater temperature. For each model, the correlation coefficient r^2 is indicated. Two clusters are displayed: riverine-influenced environments (dark gold) or open marine (blue) environments. In the models from Tynan et al. (2017), MB refers to the Moreton Bay and PL to Pambula Lake.

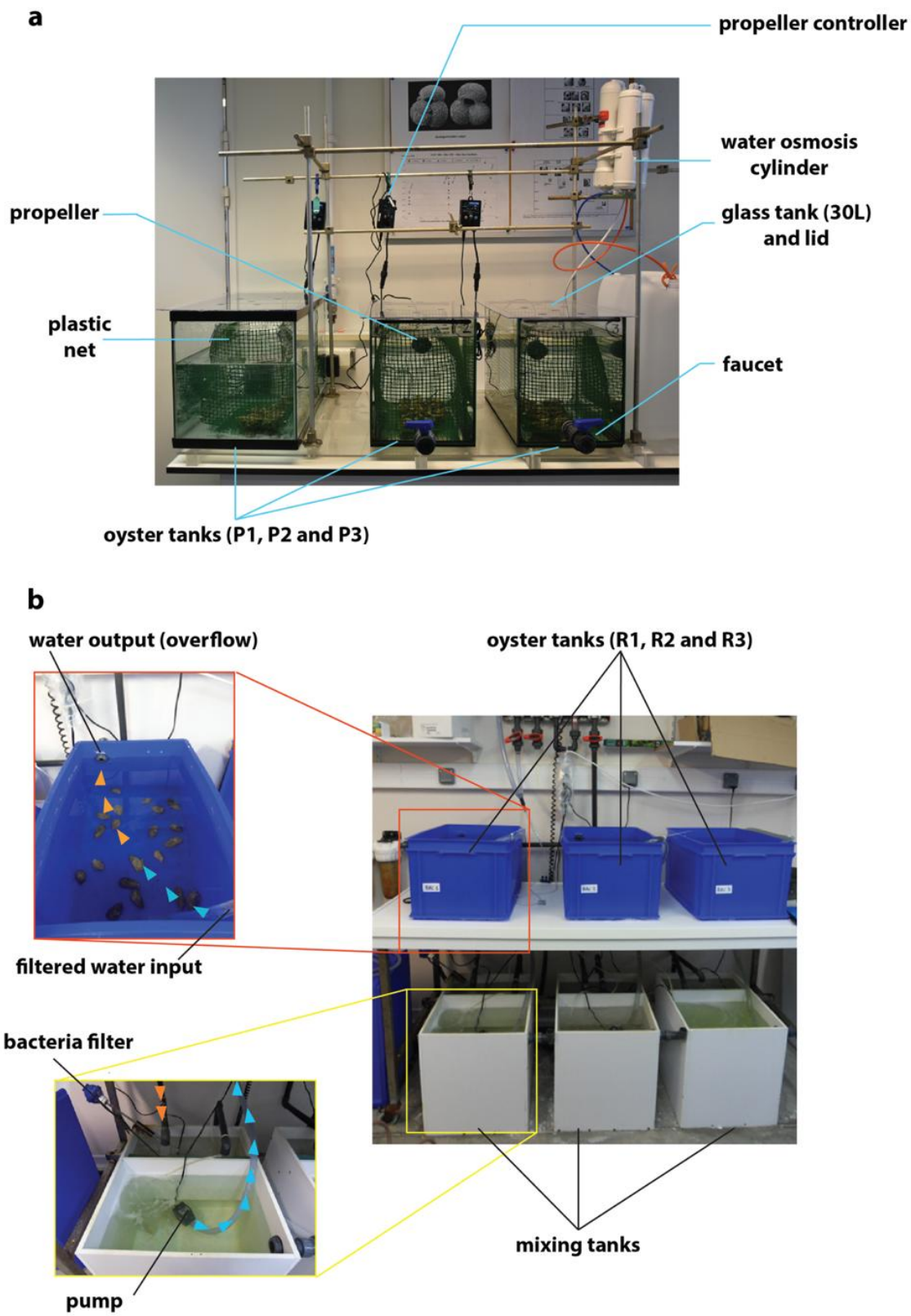

1042
1043

1044 **Figure 2: Experimental settings at Paris (a) and Roscoff (b).**

1045

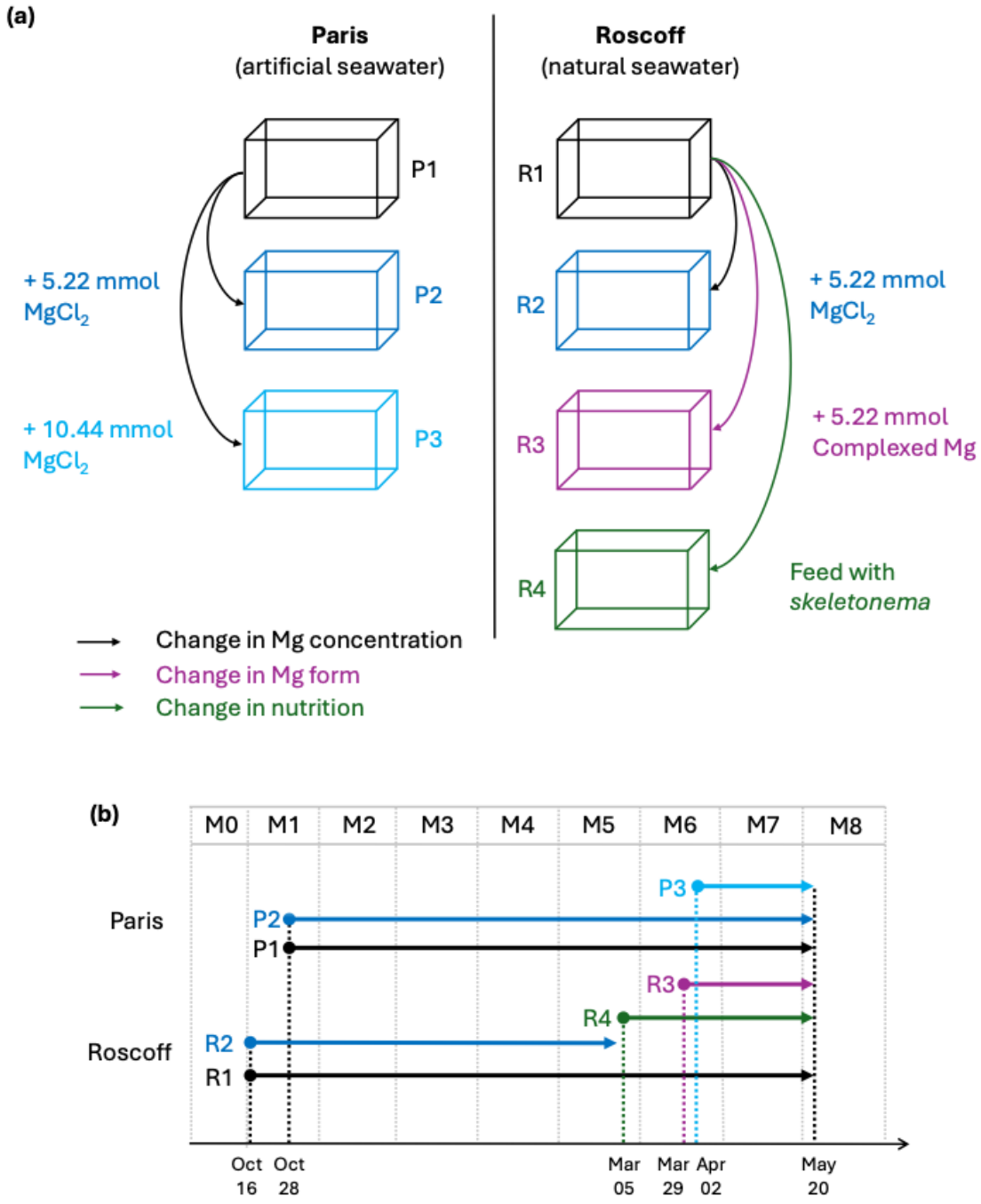

Figure 3: Summary of experimental oyster rearing conditions. (a) Schematic diagram of experimental rearing conditions at the Paris and Roscoff sites. **(b)** Gantt chart showing the timing and duration of experimental conditions applied to *M. gigas* rearing tanks. The upper time axis is divided into intervals representing months of the experiment (M1, M2, etc.), where M0 corresponds to the adaptation period *of M.gigas* to the culture conditions.

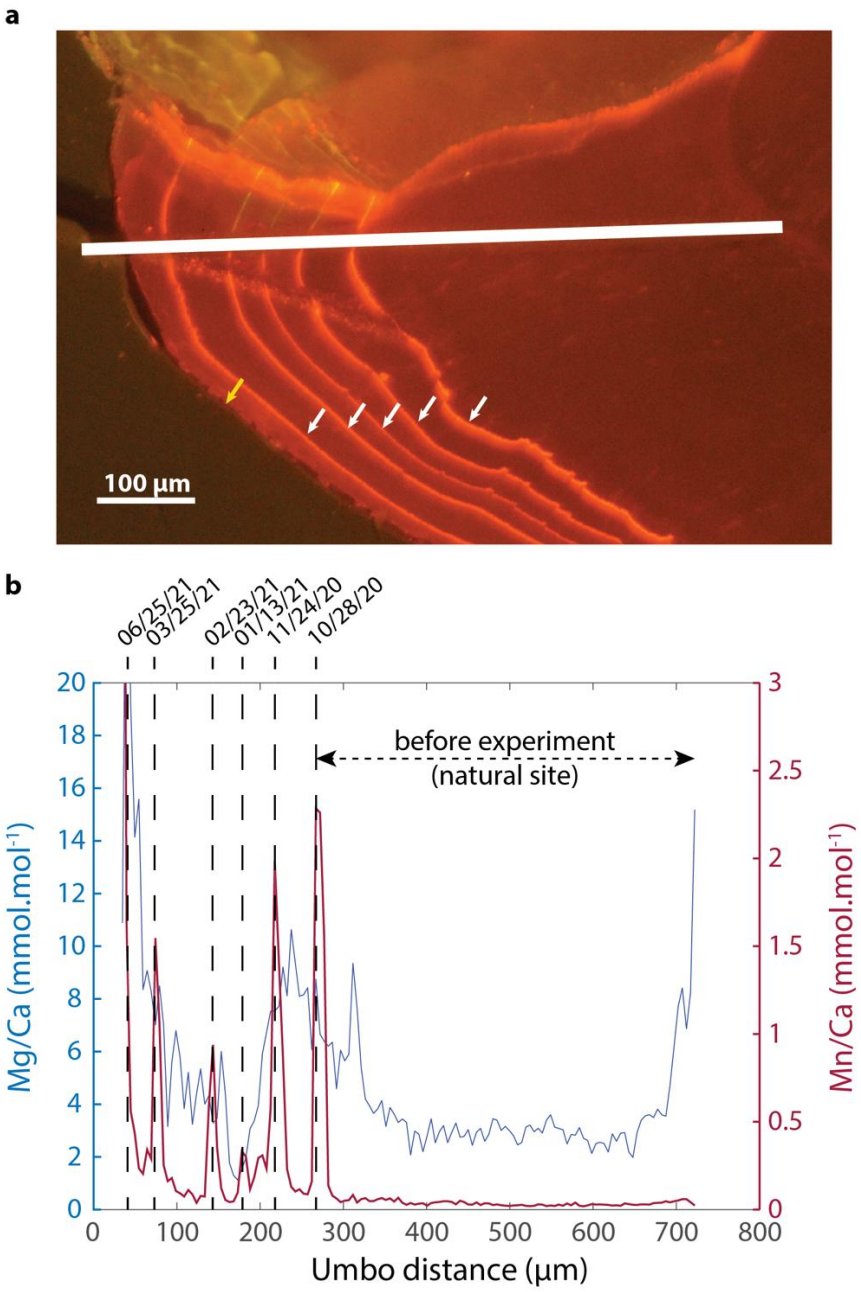

Figure 4: **Mn-labels in specimen G-308**. **a:** Cathodoluminescence image of the thin section showing the final portion of shell growth during rearing experiment. Mn-labels are indicated by white arrows, and the end of life is marked by the yellow arrow. The last Mn-label is not visible here due to low growth rate between this label and the end of life. The location of the LA-ICP-MS transect is shown by the white line. **b:** LA-ICP-MS transect of Mg/Ca and Mn/Ca ratios along the direction indicated in panel (**a**). The dates of all Mn-labels are indicated, based on the Mn/Ca variations.

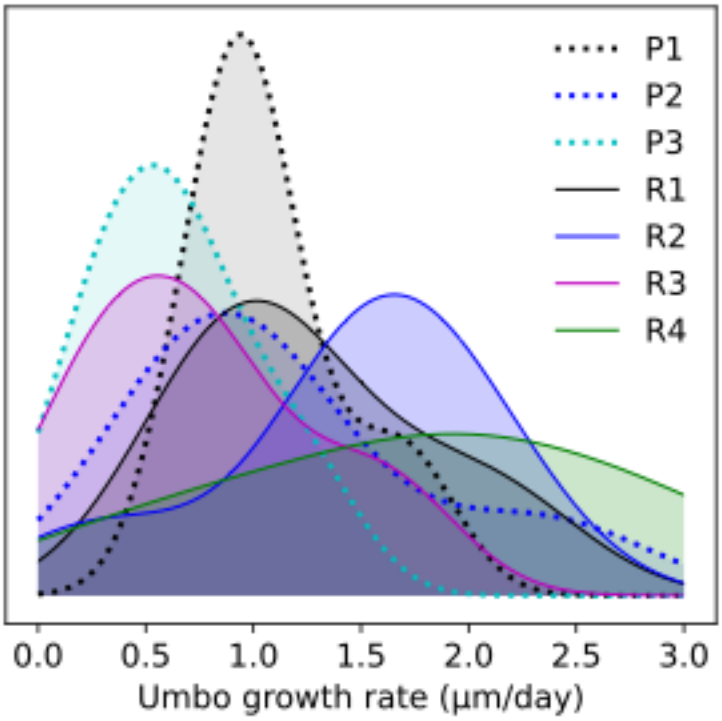

Figure 5: Comparison of oyster (umbo) growth rate distributions across experimental conditions using kernel density estimation (KDE).

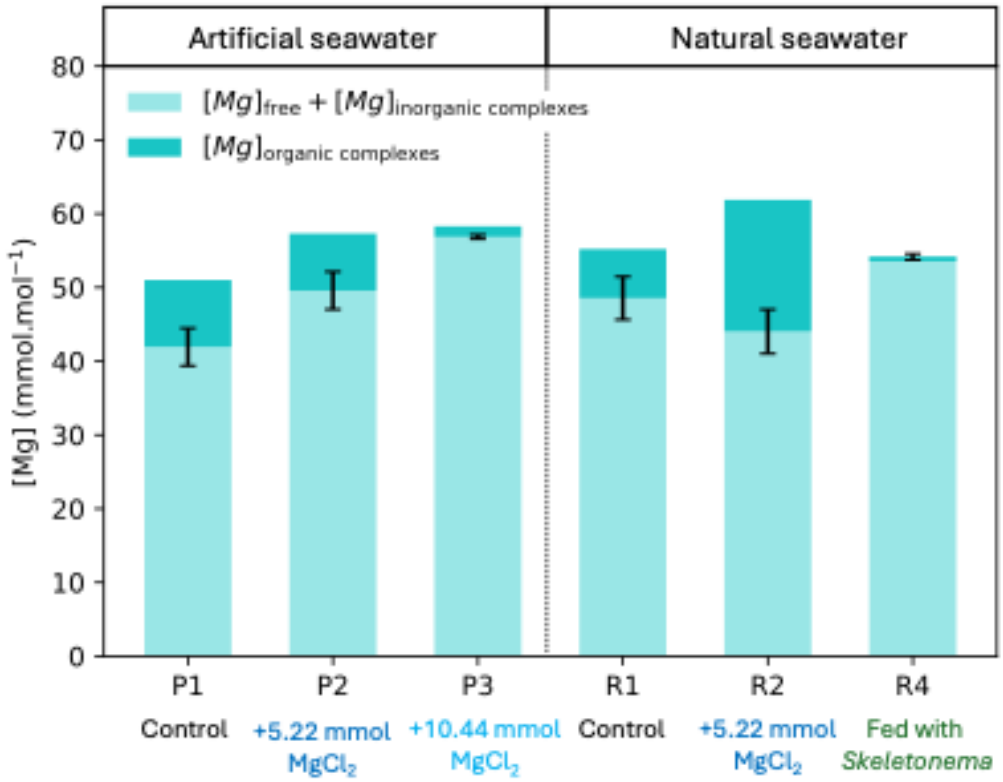

Figure 6: Proportions of complexed Mg with organics (dark blue) compared to free Mg + complexed Mg with inorganic (light blue) in seawater across oyster rearing conditions.

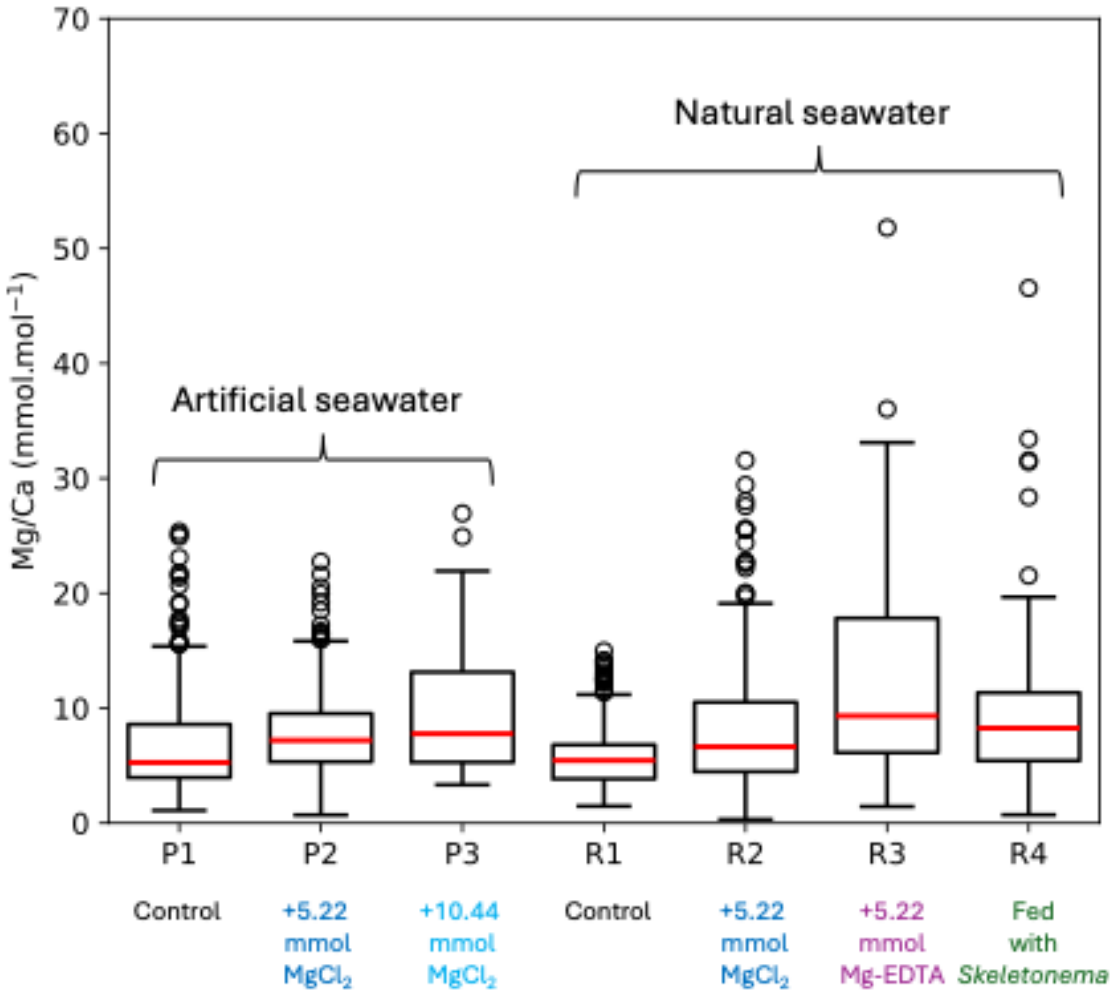

Figure 7: Boxplot of shell Mg/Ca for all experimental conditions. Different letters above the boxplots indicate statistically significant differences among groups (Tukey test).

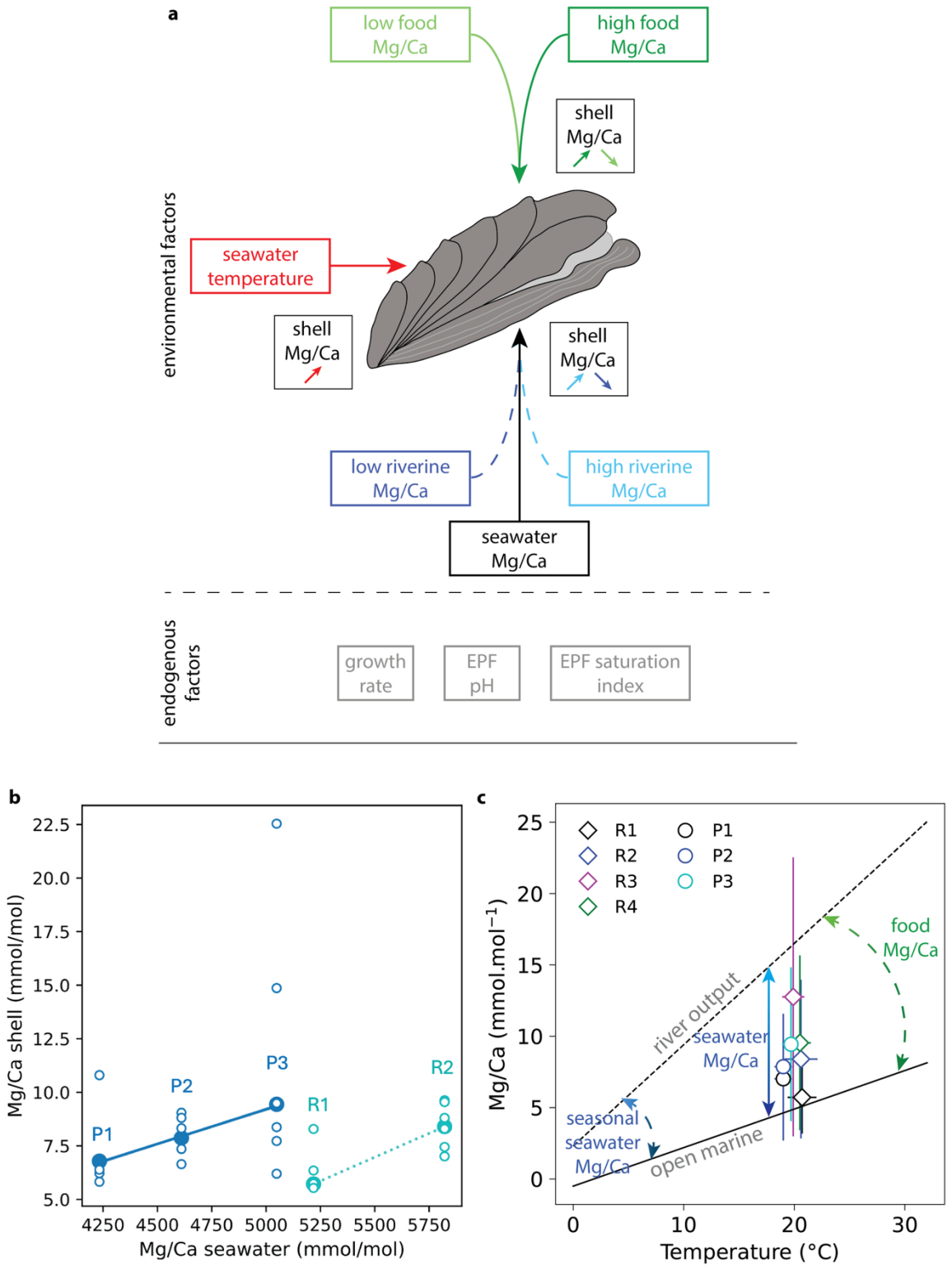

Figure 8: a) Schematic summary of environmental and physiological (endogenous) factors influencing bivalve shell Mg/Ca ratios, based on previous studies and data from this study. b) Shell Mg/Ca versus seawater Mg/Ca. Dark blue symbols represent *M.gigas* reared in artificial seawater (Paris), while light blue symbols represent *M.gigas* reared in natural seawater (Roscoff). For each experimental condition,

white filled dots indicate the median shell Mg/Ca per individual. Wolor filled dots represent the median shell Mg/Ca per experimental condition. c) Suggested effect of seawater and food Mg/Ca on Mg/Ca – T models.

Table 1: **Number of specimens analysed by LA-ICP-MS and total analytical measurements per experimental condition.** ASW: artificial seawater; NSW: natural seawater.

Experimental conditions		Number of measured specimens	Total number of measurements
P1	ASW, control	4	350
P2	ASW, +5.22 mmol $MgCl_2$	5	325
P3	ASW, +10.44 mmol $MgCl_2$	6	60
R1	NSW, control	5	415
R2	NSW, +5.22 mmol $MgCl_2$	6	268
R3	NSW, +10.44 mmol Mg-EDTA	5	165
R4	NSW, diet change	9	51

Table 2: Summary of seawater and shell measurements for all experimental conditions.

	Seawater				Shells		
Condition	Temperature (°C)	Salinity (psu)	Mg/Ca ($mmol.mol^{-1}$)	$[Mg]_{organic\ complexed}/[Mg]_{tot}$ (%)	Umbo growth rate (µm/day)	Average Mg/Ca ($mmol.mol^{-1}$)	Log D_{Mg}
P1	19.0±0.8	35±2	4233.2±0.6	17.8 ± 6.0	1.09±0.40	6.79±4.45	-2.78
P2	19.0±0.8	36±1	4610.6±1.3	13.4 ± 6.3	1.16±0.69	7.87±3.71	-2.77
P3	19.7±0.8	35±1	5048.6±0.8	2.4 ± 1.8	0.64±0.38	9.44±5.39	-2.73
R1	20.7±1.3	-	5218.3±0.2	12.1 ± 5.6	1.41±0.98	5.72±2.54	-2.96
R2	20.6±1.5	-	5821.3	28.9 ± 4.8	1.43±0.83	8.40±5.56	-2.84
R3	19.9±1.0	-	5394.1±0.4	-	0.73±0.51	12.76±9.77	-2.63
R4	20.5±1.0	-	5236.6	0 ± 0.8	1.77±0.96	9.54±6.12	-2.74

Table 3: Total Ca and Mg concentration (mmol) measured by ICP-OES and free Mg concentration measured by IC in oyster rearing seawater. Concentrations are shown for each condition as the mean of all samples analyzed over the rearing period. The associated standard errors are given at 1σ.

Conditions		ICP-OES			IC		ICP-OES - IC
		N	$[Ca]_{tot}$ (mmol)	$[Mg]_{tot}$ (mmol)	N	$\sum([Mg]_{free}, [Mg]_{inorganic\ complexe}$ (mmol)	$[Mg]_{organic\ complexe}$ (mmol)
P1	ASW	14	12.05 ± 0.22	51.01 ± 0.66	2	41.93 ± 2.55	9.08 ± 2.63
P2	ASW	14	12.43 ± 0.22	57.31 ± 1.32	2	49.58 ± 2.55	7.73 ± 2.87
P3	ASW	8	11.55 ± 0.24	58.30 ± 0.82	1	56.86 ± 0.29	1.44 ± 0.87
R1	NSW	2	10.58 ± 0.17	55.21 ± 0.21	2	48.55 ± 2.92	6.66 ± 2.92
R2	NSW	1	10.63	61.88	1	44.02 ± 3.00	17.86 ± 3.00
R3	NSW	3	10.58 ± 0.14	57.07 ± 0.45	0	Not analized	
R4	NSW	1	10.23	53.57	1	54.15 ± 0.41	0 ± 0.41

Table 4: Description of shell Mg/Ca (in $mmol.mol^{-1}$) according to condition. Number of individuals corresponds to the number of analyzed oysters in each condition.

Condition	Number of individuals	Mean Mg/Ca	Median Mg/Ca	Standard deviation	Minimum Mg/Ca	Maximum Mg/Ca
P1	4	6.79	5.26	4.45	1.10	25.37
P2	5	7.87	7.19	3.71	0.70	22.74
P3	6	9.44	7.78	5.39	3.33	26.94
R1	5	5.72	5.45	2.54	1.47	14.98
R2	6	8.40	6.64	5.56	0.31	31.56
R3	5	12.76	9.32	9.77	1.44	51.80
R4	9	9.54	8.26	6.12	0.71	46.55

Supplementary Data 1 on "Evidence for seawater Mg/Ca and dietary control on Mg incorporation in oyster shells"

Marie Pesnin[1,2*], Laurent Emmanuel[2], Amélie Guittet[2], Boris Eyheraguidel[3], Gaëtan Schires[4], Julien Normand[5], Vincent Mouchi[6]

[1]: Geowissenschaftliches Zentrum, Georg–August–Universität Göttingen, 37077, Göttingen, Germany.

[2]: Sorbonne Université, CNRS-INSU, Institut des Sciences de la Terre Paris, ISTeP, F-75005, Paris, France

[3]: Institut de Chimie de Clermont-Ferrand, Campus universitaire des Cézeaux, 63178, Aubière, France

[4]: Station Biologique de Roscoff, CNRS-Sorbonne Université, Roscoff 29682, France.

[5]: Ifremer, Laboratoire Environnement Ressources de Normandie, Avenue du Général de Gaulle, 14520, Port-en-Bessin, France

[6]: CNRS, CReAAH, Université de Rennes, Campus Beaulieu, 263 avenue Général Leclerc, 35042, Rennes Cedex, France

*Corresponding author: marie.pesnin@uni-goettingen.de

*Corresponding author: marie.pesnin@uni-goettingen.de

1. Labelled oyster shell from the rearing experiment

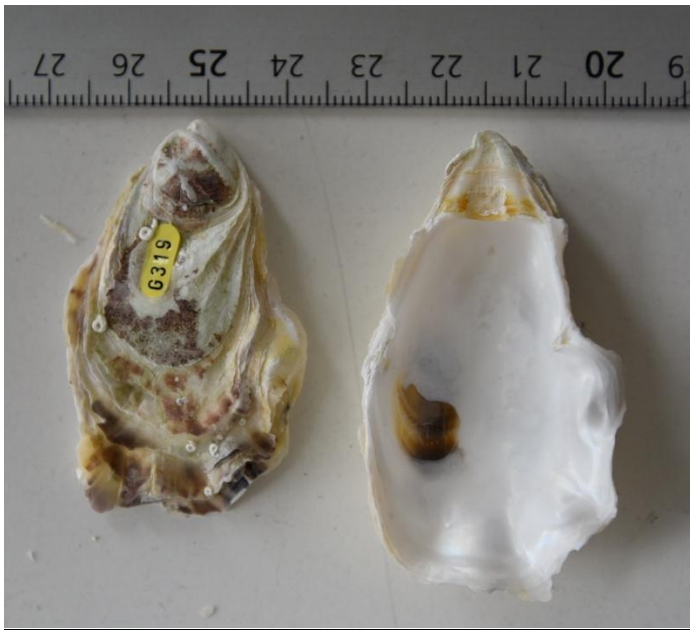

Figure S1: Picture of the shell of one oyster specimen G.319 reared in artifical seawater sacrificed for geochemical measurements after removing the soft tissue from the organism and cleaning the shell from organic residute with oxygen peroxyde.

2. Monitoring of physicochemical parameters of seawater in rearing tanks

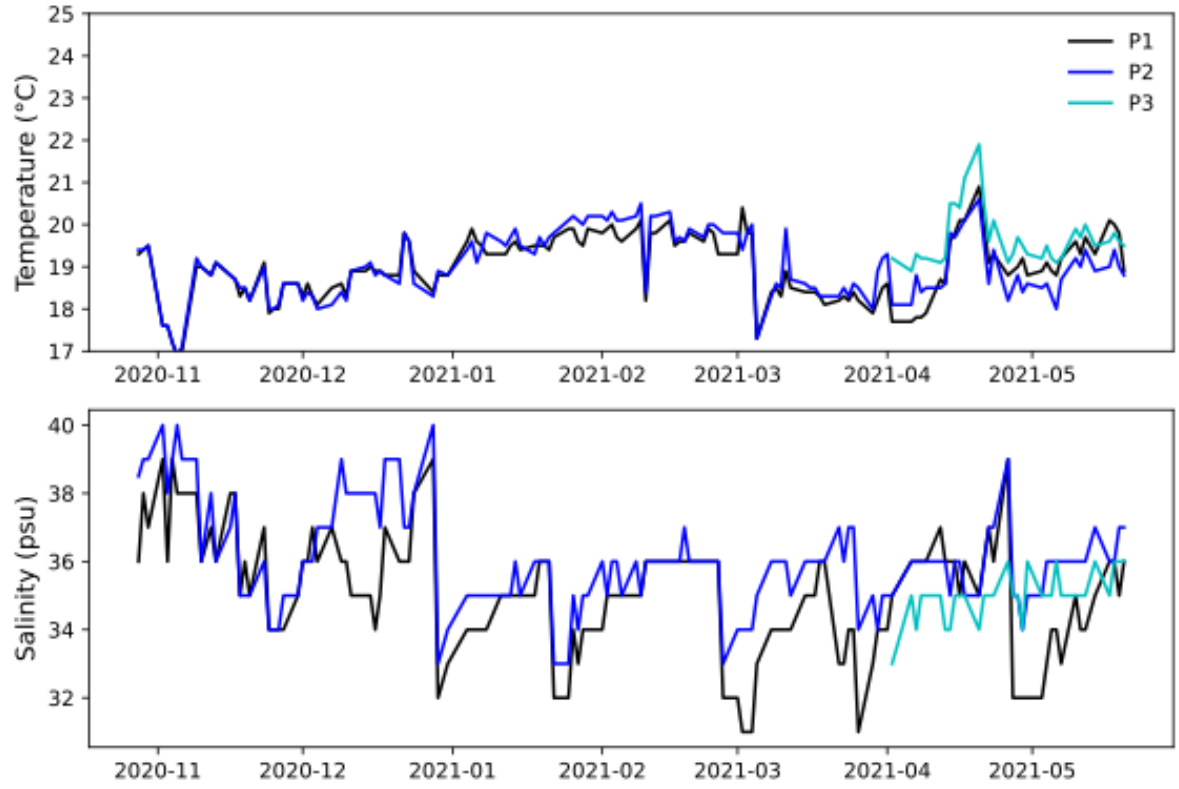

Figure S2: Daily recording of temperature (°C), salinity (‰) of artificial seawater in aquariums as a function of culture conditions.

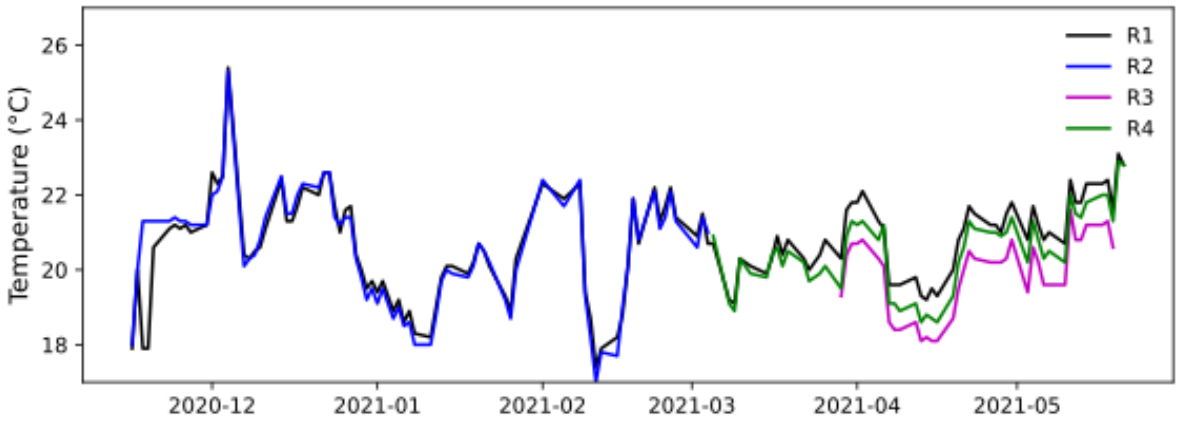

Figure S3: Daily recording of temperature (°C) natural seawater in aquariums as a function of culture conditions.

3. Growth rate and mortality of *M. gigas* over the culture experiment

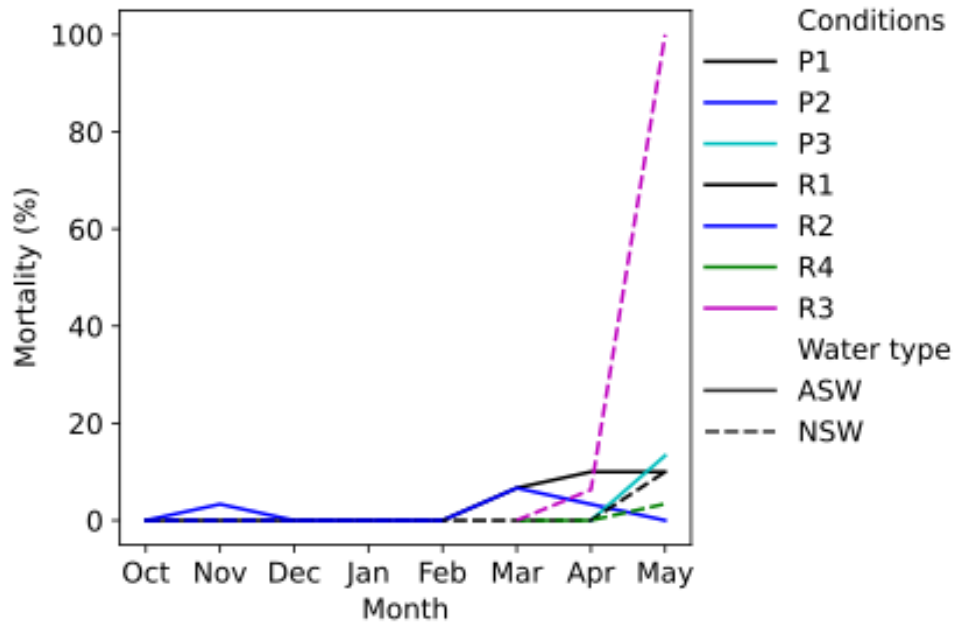

Figure S4: Monitoring of *M. gigas* mortality over rearing experiment.

Table S1: Growth rate of *M. gigas* oyster umbo under culture conditions, determined from cathodoluminescence observations.

ID	Conditions	Starting date	End date	Total days	Umbo length (µm)	Growth rate (µm/day)
G.302	P1	28/10/2020	24/05/2021	208	196,7	0,95
G.308	P1	28/10/2020	15/07/2021	260	204,0	0,78
G.314	P1	28/10/2020	11/06/2021	226	220,0	0,97
G.324	P1	28/10/2020	19/05/2021	203	341,2	1,68
G.333	P2	28/10/2020	23/07/2021	268	276,2	1,03
G.334	P2	28/10/2020	24/05/2021	208	139,5	0,67
G.352	P2	28/10/2020	15/07/2021	260	277,5	1,07
G.355	P2	28/10/2020	24/05/2021	208	143,1	0,69
G.360	P2	28/10/2020	24/05/2021	208	487,2	2,34
G.365	P3	02/04/2021	26/07/2021	115	20,4	0,18
G.373	P3	02/04/2021	29/07/2021	118	75,7	0,64
G.375	P3	02/04/2021	08/05/2021	36	12,8	0,35
G.383	P3	02/04/2021	08/05/2021	36	30,8	0,85
G.374	P3	02/04/2021	24/05/2021	52	28,7	0,55
G.388	P3	02/04/2021	24/05/2021	52	64,3	1,24
G.075	R1	16/10/2020	29/03/2021	164	125,6	0,77
G.054	R1	16/10/2020	29/03/2021	164	157,1	0,96
G.096	R1	16/10/2020	19/05/2021	215	270,6	1,26

G.129	R1	16/10/2020	29/03/2021	164	341,6	2,08
G.032	R1	16/10/2020	19/05/2021	215	650,9	3,03
G.124	R1	16/10/2020	17/05/2021	213	78,2	0,37
G.071	R2	16/10/2020	29/03/2021	164	266,8	1,63
G.116	R2	16/10/2020	29/03/2021	164	302,5	1,84
G.012	R2	16/10/2020	05/03/2021	140	24,4	0,17
G.053	R2	16/10/2020	05/03/2021	140	40,3	0,29
G.056	R2	16/10/2020	29/03/2021	164	230,1	1,40
G.087	R2	16/10/2020	05/03/2021	140	297,0	2,12
G.127	R2	16/10/2020	05/03/2021	140	203,6	1,45
G.013	R3	29/03/2021	10/05/2021	42	63,3	1,51
G.055	R3	29/03/2021	10/05/2021	42	5,9	0,14
G.071	R3	29/03/2021	10/05/2021	42	35,4	0,84
G.075	R3	29/03/2021	09/05/2021	41	18,2	0,44
G.116	R3	29/03/2021	09/05/2021	41	34,3	0,84
G.054	R3	29/03/2021	19/05/2021	51	12,0	0,24
G.056	R3	29/03/2021	19/05/2021	51	21,7	0,43
G.127	R3	29/03/2021	17/05/2021	49	81,1	1,66
G.129	R3	29/03/2021	17/05/2021	49	39,0	0,80
G.016	R3	29/03/2021	10/05/2021	42	19,1	0,46
G.012	R4	05/03/2021	19/05/2021	75	41,5	0,55
G.053	R4	05/03/2021	19/05/2021	75	214,8	2,86
G.087	R4	05/03/2021	19/05/2021	75	121,6	1,62
G.016	R4	05/03/2021	29/03/2021	24	48,6	2,03

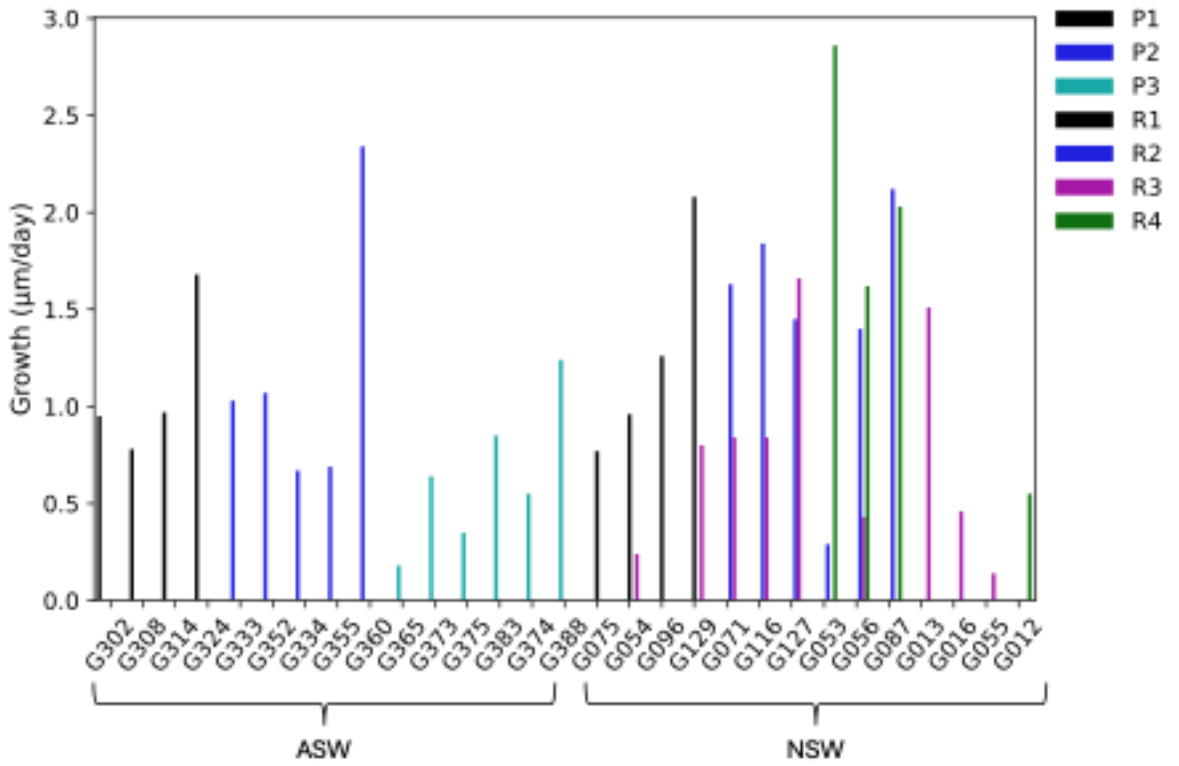

Figure S5: Growth rate of the umbo in M. gigas oysters throughout the experimental period, per individual.

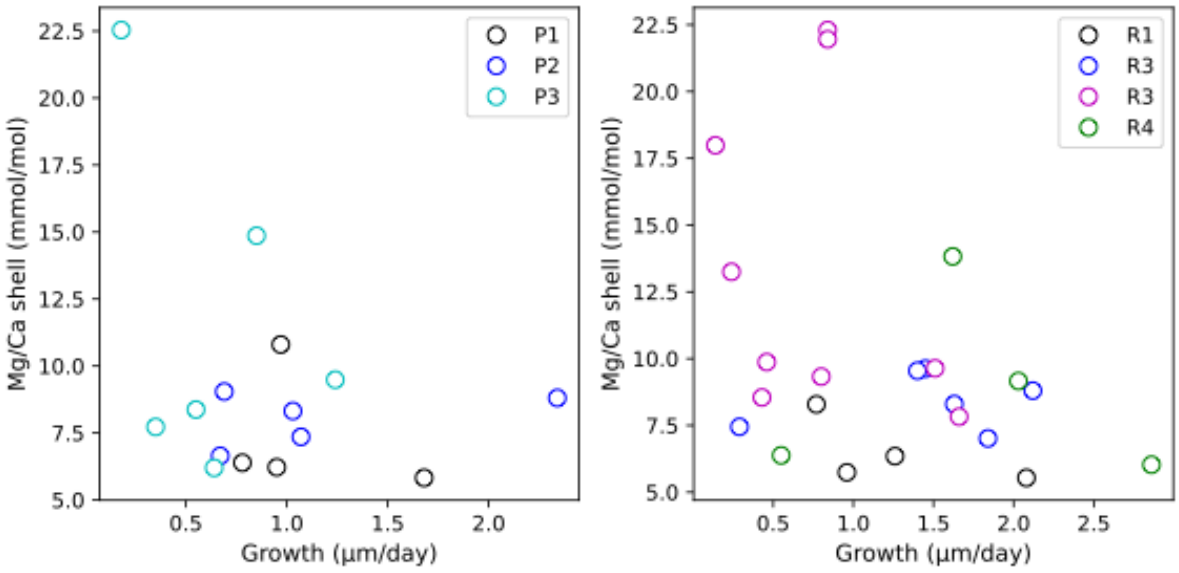

Figure S6: Comparison of individual mean shell Mg/Ca ratios with umbo growth rates.

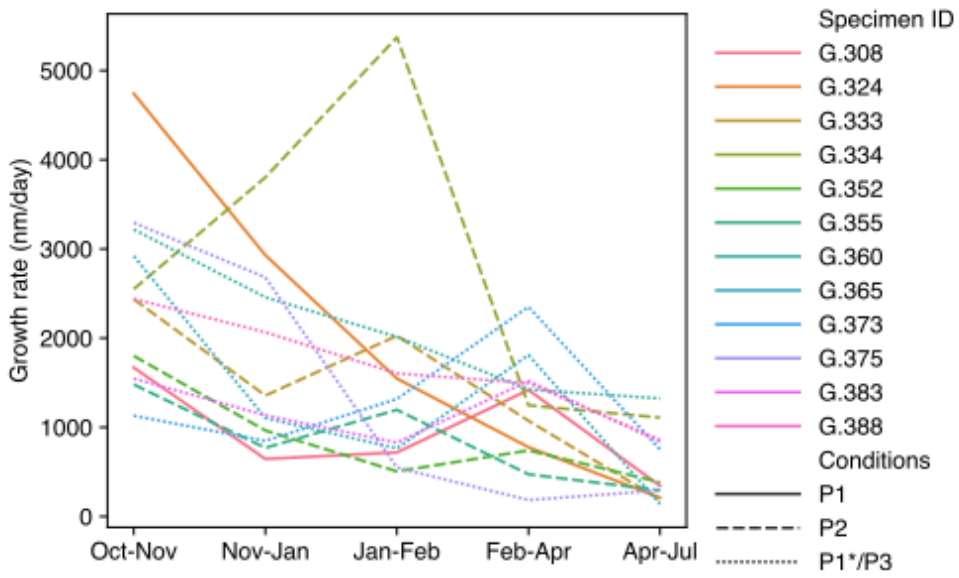

Figure S7: Evolution of the growth rate on the umbo of *M. gigas* specimens raised in artificial seawaters along the culture experiment.

4. Experimental conditions for all analysed specimens

Table S2: Oyster specimens analysed by LA-ICP-MS and their respective experimental conditions during the experiment. Some specimens have been transferred during the experiment from one condition to another, after *in vivo* Mn-labelling.

ID	*Conditions*
G.012	R4
G.013	R3
G.016	R1, R3
G.053	R2, R4
G.054	R1, R3
G.055	R3
G.056	R2, R4, R3
G.071	R2, R3
G.075	R1
G.087	R2, R4
G.096	R1
G.116	R2, R3
G.127	R2, R3
G.129	R1, R3
G.302	P1
G.308	P1
G.314	P1
G.324	P1
G.333	P2
G.334	P2
G.352	P2
G.355	P2
G.360	P2
G.365	P3
G.373	P3
G.374	P3

G.375	P3
G.383	P3
G.388	P3

5. Comparison of shell Mg/Ca between analytical platforms

Table S3: Results for Kruskal-Wallis tests performed to test the null hypothesis that, for each experimental condition measured at both analytical platforms (CReAAH and IPREM), the shell Mg/Ca comes from the same distribution.

Conditions	***p-value***
P1	0.0851
P2	0.3299
P3	0.3804
R1	0.0119
R2	0.1105
R4	0.0722
R3	0.1218

6. Impact of seawater renewal on Mg concentration in seawater

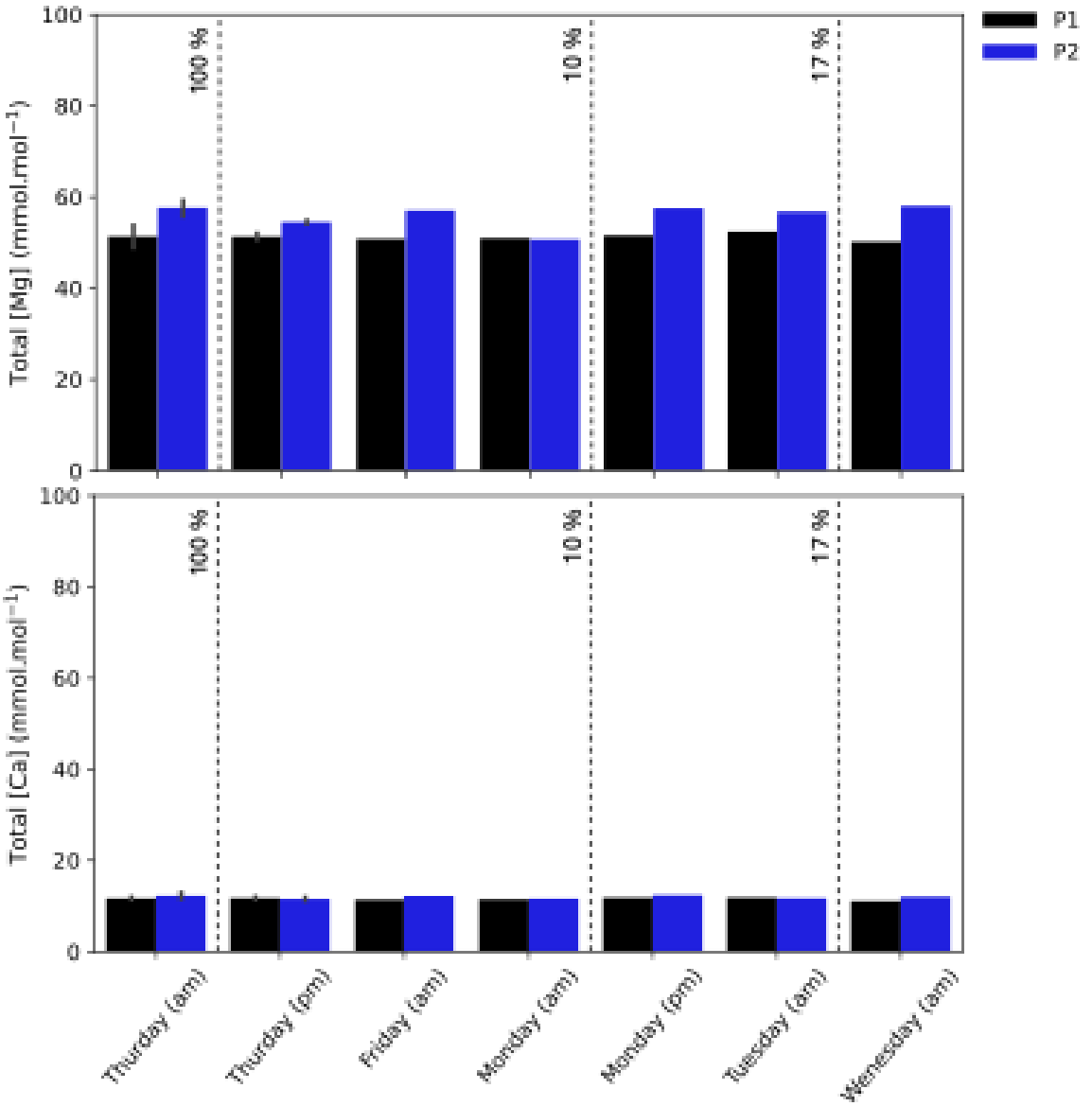

Figure S8: Daily evolution of calcium (top panel) and magnesium (bottom panel) concentrations in P1 (dark bars) and P2 (blue bars) aquaria before (am) and after (pm) seawater renewal. The percentage corresponds to the percentage of renewed water in the aquariums.

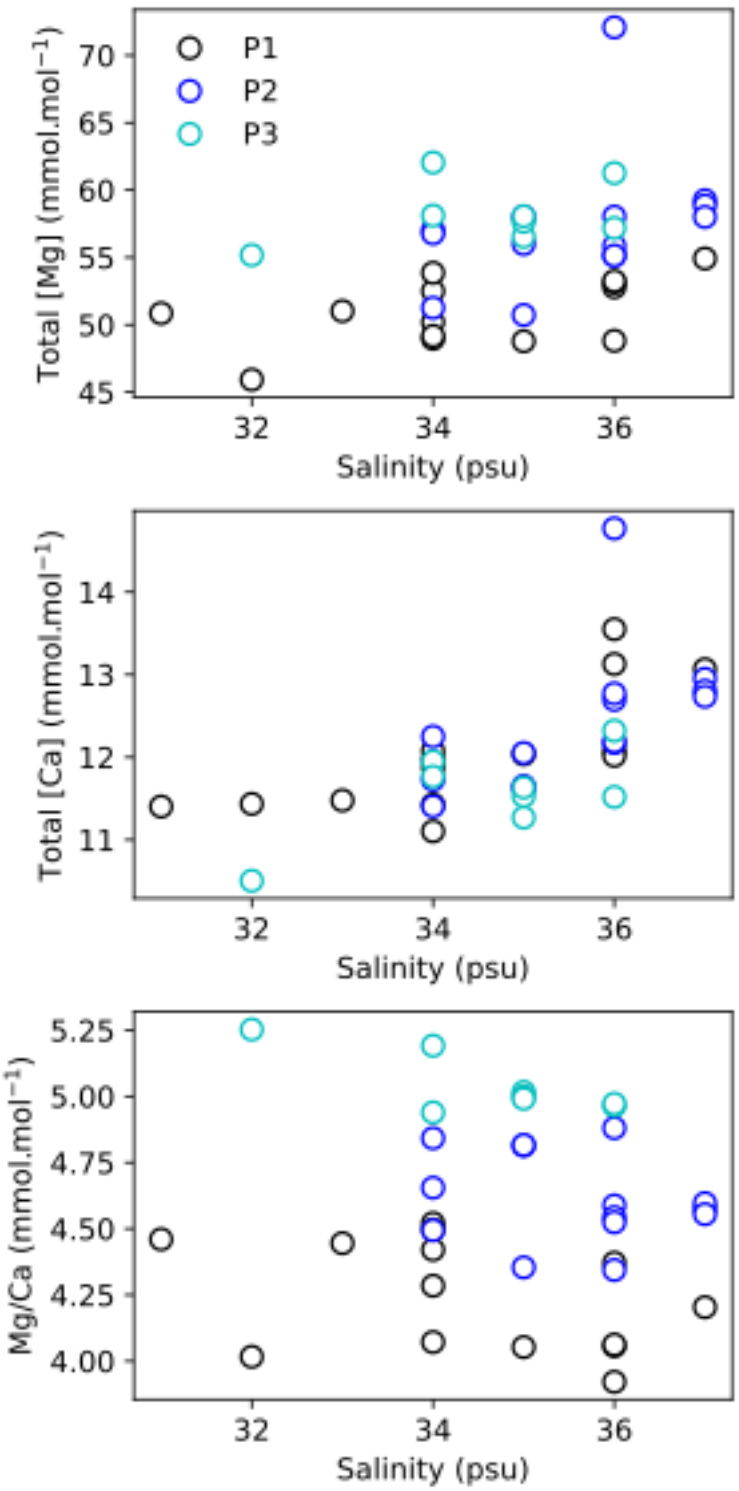

Figure S9: Evolution of [Ca], [Mg] and Mg/Ca ratio of the artificial seawater sampled from P1, P2 en P3 conditions as function of salinity

7. Impact of seawater Mg enrichment on reconstructed temperatures

We present here the reconstructed temperatures by several thermodependant Mg/Ca models from oysters (Surge & Lohmann, 2008; Mouchi et al., 2013; Tynan et al., 2017) and mussels (Klein et al., 1996; Vander Putten et al., 2000; Freitas et al., 2008) from our natural (NSW: R1-R4) and artificial (ASW: P1-P3) seawater experiments. As seawater Mg/Ca is different between both experiments, comparisons should be made separately. For the study from Tynan et al. (2017), we used the equation from Moreton Bay as it corresponds to marine settings, which fit better to our experimental setup.

Table S4: Reconstructed temperatures from shell Mg/Ca of this study based on models from the literature. Differences (in °C) from control (P1 and R1 conditions) are indicated under brackets.

	P1	**P2**	**P3**	**R1**	**R2**	**R3**	**R4**
Shell Mg/Ca (mmol.mol^{-1}) [difference from control]	7.02 [-]	7.87 [0.85]	9.44 [2.42]	5.72 [-]	8.40 [2.68]	12.76 [7.04]	9.54 [3.82]
Reconstructed temperature – Klein et al. (1996): T = (Mg/Ca - 2.25) / 0.3 [difference from control]	15.9°C [-]	18.7°C [2.8°C]	24.0°C [8.1°C]	11.6°C [-]	20.5°C [8.9°C]	35.0°C [23.4°C]	24.3°C [12.7°C]
Reconstructed temperature – Vander Putten et al. (2000): T = (Mg/Ca + 0.63) / 0.7 [difference from control]	10.9°C [-]	12.1°C [1.2°C]	14.4°C [3.5°C]	9.1°C [-]	12.9°C [3.8°C]	19.1°C [10.0°C]	14.5°C [5.4°C]
Reconstructed temperature – Freitas et al. (2008): T = (Mg/Ca – 1.503) / 0.265 [difference from control]	20.8°C [-]	24.0°C [3.2°C]	30.0°C [9.2°C]	15.9°C [-]	26.0°C [10.1°C]	42.5°C [26.6°C]	30.3°C [14.4°C]
Reconstructed temperature – Surge & Lohmann (2008): T = (Mg/Ca + 0.23) / 0.72 [difference from control]	10.1°C [-]	11.3°C [1.2°C]	13.4°C [3.3°C]	8.3°C [-]	12.0°C [3.7°C]	18.0°C [9.7°C]	13.6°C [5.3°C]
Reconstructed temperature – Mouchi et al. (2013): T = (Mg/Ca * 3.77) + 1.88 [difference from control]	28.3°C [-]	31.5°C [3.2°C]	37.5°C [9.2°C]	23.4°C [-]	33.5°C [10.1°C]	50.0°C [26.6°C]	37.8°C [14.4°C]
Reconstructed temperature – Tynan et al. (2017) Moreton Bay: T = (Mg/Ca - 2.31) / 0.71 [difference from control]	6.6°C [-]	7.8°C [1.2°C]	10.0°C [3.4°C]	4.8°C [-]	8.6°C [3.8°C]	14.7°C [9.9°C]	10.2°C [5.4°C]